

TOPICAL REVIEW • OPEN ACCESS

External-field-assisted additive manufacturing for micro/nano device fabrication

To cite this article: Bin Wang *et al* 2026 *Int. J. Extrem. Manuf.* **8** 012005

View the [article online](#) for updates and enhancements.

You may also like

- [Metal-organic frameworks for gas sensors: comprehensive review from principal fabrication to application](#)
Soon Hyeong So, Seung Yong Lee, Hohyung Kang et al.
- [Neuromorphic devices for intelligent visual perception](#)
Yixin Zhu, Xiangjing Wang, Yuqing Hu et al.
- [Memristor devices for next-generation computing: from performance optimization to application-specific co-design](#)
Zhaorui Liu, Caifang Gao, Jingbo Yang et al.

Topical Review

External-field-assisted additive manufacturing for micro/nano device fabrication

Bin Wang¹, Jiansheng Du¹, Haoyu Zhang¹, Ying Cao¹, Chengyu Wen¹,
Veronica Iacovacci³, Zhiyang Lyu^{1,*} , Tianlong Li^{2,*}  and Qianqian Wang^{1,*} 

¹ Jiangsu Key Laboratory for Design and Manufacturing of Precision Medicine Equipment, School of Mechanical Engineering, Southeast University, Nanjing 211189, People's Republic of China

² State Key Laboratory of Robotics and Systems, Harbin Institute of Technology, Harbin 150001, People's Republic of China

³ The BioRobotics Institute, Department of Excellence in Robotics and AI, Scuola Superiore Sant'Anna, Pisa 56127, Italy

E-mail: zhiyanglyu@seu.edu.cn, tianlongli@hit.edu.cn and qqwang@seu.edu.cn

Received 28 March 2025, revised 31 May 2025

Accepted for publication 19 September 2025

Published 9 October 2025



Abstract

Micro/nano devices (MNDs) are characterized by miniaturization, high precision, and multifunctional integration, making them highly suitable for use in areas such as microrobotics, biomedical devices and electronic sensors. Their fabrication requires exceptional precision in structural integrity, material control, and functional integration. Traditional micro/nano fabrication techniques face inherent limitations in constructing complex three-dimensional (3D) architectures and integrating multiple materials. While additive manufacturing (AM) provides flexibility, challenges remain in material alignment control, microstructural organization, and multifunctional integration. To overcome these limitations, field-assisted additive manufacturing (FAM) has emerged as a promising approach that combines magnetic, acoustic, or electric fields to regulate material alignment, microstructural organization, and spatial alignment. This capability improves fabrication precision, enhances material anisotropy and facilitates functional integration. This review systematically explores the mechanisms, fabrication process, and functional integration of FAM in the framework of nozzle-based and vat photopolymerization-based, while further exploring their applications in microrobotics, biomedical devices, and electronic sensors. Moreover, this review provides a comparative overview of different FAM approaches, highlighting their respective characteristics, typical applications, and unique advantages. In addition, the major challenges facing FAM research are comprehensively assessed and future directions are explored, including advances in spatial

* Authors to whom any correspondence should be addressed.



Original content from this work may be used under the terms of the [Creative Commons Attribution 4.0 licence](https://creativecommons.org/licenses/by/4.0/). Any further distribution of this work must maintain attribution to the author(s) and the title of the work, journal citation and DOI.

precision control capability, intelligent control for process integration, and multi-field coupling optimization. This review establishes a foundational theoretical framework that can serve as a systematic reference for micro/nano manufacturing researchers to promote the development of FAM for high-performance micro/nano device fabrication.

Keywords: additive manufacturing, 3D printing, field-assisted additive manufacturing, micro/nano devices

1. Introduction

Micro/nano devices (MNDs) play a crucial role in biomedical engineering^[1–3], electronics^[4–7], and microrobotics^[8–11], with their miniaturization, high precision, and functional integration making them a key research focus in micro/nano manufacturing^[12,13]. These devices typically feature highly complex three-dimensional (3D) microstructures and require the integration of multiple functional materials at extremely small scales to meet different application requirements^[14,15]. The fabrication of MNDs not only necessitates precise geometric control but also demands uniform material distribution at the microscale or nanoscale and stable physicochemical properties to ensure the desired functional characteristics^[16,17]. In addition, with the growing demand for intelligent and multifunctional devices, manufacturing process must meet advanced integration requirements, including flexible deformability, programmable responses, and precise control, which poses even greater challenges to fabrication methods^[18–20]. However, achieving high-performance devices at the micro- and nanoscale remains challenging, particularly in terms of improving fabrication resolution, optimizing material manipulation, and enhancing device stability^[21–23].

Traditional micro/nano manufacturing methods have been widely used in various high-precision fabrication fields^[24], and they have shown significant value, especially in the field of microelectronics^[25,26], biosensing^[27,28], and micro electro mechanical systems^[29,30]. However, these methods are primarily suited for producing regular and relatively simple structures, and they face considerable limitations when dealing with MNDs featuring complex 3D topologies and highly integrated functional materials. The core challenges include material processing compatibility, constraints in structural design freedom, and difficulties in precisely controlling material assembly and orientation at the microscale^[15,31,32]. In particular, for the fabrication of anisotropic micro/nano structures and multifunctionally integrated devices, conventional methods are limited by fixed processing modes and material choices, making it difficult to achieve spatial programmability of material properties. This limits their application in advanced manufacturing^[33,34].

Additive manufacturing (AM) has introduced an innovative approach to the fabrication of complex micro/nano structures through a layer-by-layer construction strategy^[35–37]. Unlike conventional subtractive and formative manufacturing techniques, AM offers higher geometric freedom,

enabling the production of highly intricate 3D structures. At the same time, AM also provides advantages such as reduced material waste and improved manufacturing efficiency^[38,39]. In recent years, the rapid advancement of micro/nano AM has led to the emergence of several high-precision AM techniques, including two-photon polymerization (TPP)^[40], stereolithography (SLA), continuous liquid interface production (CLIP), and electrohydrodynamic jetting (EHDJ)^[41–43], peripheral photoinhibition direct laser writing (PPI-DLW), stimulated-emission depletion two-photon lithography (STED-TPL)^[44–48]. These techniques have facilitated breakthroughs in fine-feature fabrication and have been widely adopted in biomedical devices, flexible electronics, and micro-optical structures^[39,49,50].

Despite the significant potential of AM in micro/nano-scale fabrication, challenges remain in achieving precise control over functional materials and constructing complex heterogeneous structures^[33,34]. Conventional AM primarily relies on the rheological properties, melting behavior, or photopolymerization of materials for shaping, making it challenging to achieve precise local orientation control at the microscale^[51–53]. Although extrusion-based AM can utilize shear forces to guide material alignment to a certain extent, its precision and controllability remain limited. Consequently, achieving accurate local material orientation at the microscale remains a challenge, leading to fabricated devices that often exhibit isotropic characteristics, which in turn restricts their applicability in functional device manufacturing. Current AM technologies, despite achieving sufficient printing resolution^[54,55], still face critical limitations in material compatibility and interface control, particularly when applied to MNDs requiring multifunctional integration or highly complex structures. This makes it challenging to meet the stringent performance requirements of specific applications^[56,57]. Therefore, overcoming the limitations of AM in material manipulation and functional integration has become a critical direction for its further advancement.

Against this backdrop, field-assisted additive manufacturing (FAM) has emerged as a promising strategy for enhancing AM process precision and functional diversity. By incorporating external physical fields such as magnetic, acoustic, or electric fields during fabrication, FAM enables precise control over material composition, microstructural alignment, and functional properties. This approach optimizes manufacturing accuracy, enhances structural anisotropy, and improves the feasibility of multi-material integration. Recent advancements have demonstrated that external field application plays

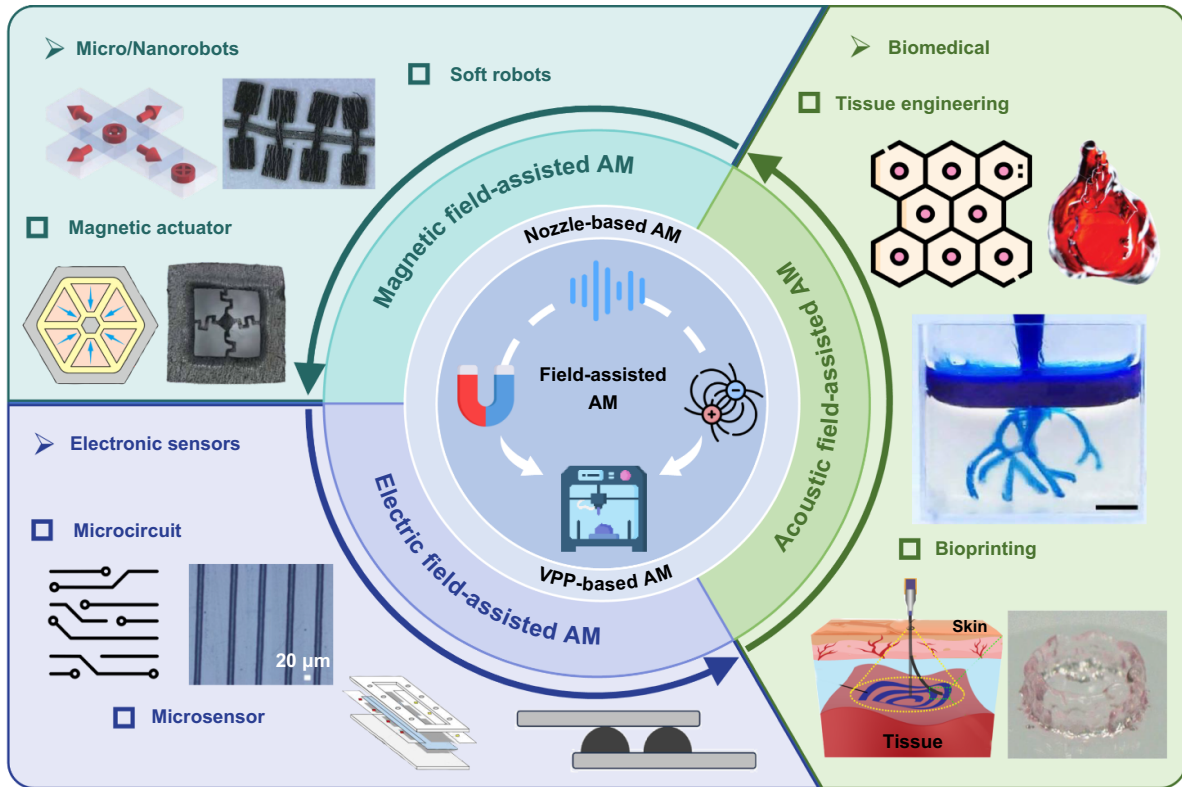


Figure 1. Integration of external fields with AM and their applications in micro/nano devices, including magnetic, acoustic, and electric fields. The insets are adapted from the following references. Soft robots. Magnetic actuator. Microcircuit. Microsensor. Tissue engineering. Bioprinting. Reproduced with permission from^[65]. CC BY-NC 4.0. From^[66]. Reprinted with permission from AAAS. Reprinted from^[67], Copyright (2024), with permission from Elsevier. Reprinted from^[68], Copyright (2024), with permission from Elsevier. Reprinted from^[69], Copyright (2022), with permission from Elsevier. Reproduced from^[70], with permission from Springer Nature. Reproduced from^[71], with permission from Springer Nature. Reproduced from^[72]. CC BY 4.0. Reproduced from^[73]. CC BY 4.0. Reproduced with permission from^[74]. CC BY-NC 4.0.

a critical role in regulating material orientation and distribution, a principle that has been widely utilized in controlling the alignment of fillers in composite materials^[58–61]. In conventional manufacturing, randomly dispersed fillers often result in isotropic material properties. However, using external fields such as magnetic^[62], acoustic^[63], and electric fields^[64], controlled filler alignment can be achieved to impart anisotropic material characteristics. Furthermore, when integrated with nozzle-based or vat photopolymerization (VPP)-based AM techniques, external fields can dynamically manipulate material orientation and movement throughout the fabrication process, ensuring greater precision in structural formation. This field-driven alignment mechanism provides a strong foundation for optimizing material orientation and microstructural control in FAM. Compared to conventional AM, FAM offers superior structural control and material manipulation, particularly at the micro/nanoscale^[52,59–63]. It holds significant potential for advancing the fabrication of micro/nanorobots, biomedical devices, and functional electronic components, enabling a novel manufacturing paradigm for high-precision, multifunctional integrated devices.

This review provides a comprehensive analysis of FAM in micro/nano fabrication, focusing on the role of magnetic, acoustic, and electric fields in improving material manipulation accuracy, structural control, and device functionality (Figure 1). Section 2 explores the fundamental principles of FAM and presents detailed discussions on magnetic field-assisted additive manufacturing (MFAM), acoustic field-assisted additive manufacturing (AFAM), and electric field-assisted additive manufacturing (EFAM), along with their specific applications in AM. Section 3 highlights FAM’s applications in microrobotics, biomedical devices, and functional electronic devices, illustrating its advantages in functional optimization and structural enhancement. Section 4 discusses current challenges in FAM, including limitations in field uniformity, process stability, and multi-field interactions, while also outlining future trends such as multi-field coupled fabrication, intelligent process optimization, and high-throughput manufacturing. By systematically reviewing the mechanisms, technological advancements, and application prospects of FAM in micro/nano device fabrication, this review aims to provide researchers with a comprehensive reference and inspire further innovations in the field.

2. Field-assisted additive manufacturing technology (FAM)

FAM is an advanced AM approach that integrates external physical fields into the AM process to enhance material control, improve fabrication precision, and impart anisotropic or stimuli-responsive functionalities to printed structures. The core principle of FAM is the integration of external physical fields to achieve synergistic regulation of material distribution, flow behavior, and curing process. This enables anisotropic functionality and dynamic response properties to be imparted to the printed structure. FAM can be categorized into MFAM, AFAM, and EFAM based on the type of external field applied. Each method offers unique advantages suited to specific manufacturing requirements. This chapter begins with an overview of AM fundamentals (Section 2.1), followed by discussions on the mechanisms, fabrication processes, and microstructural effects of MFAM (Section 2.2), AFAM (Section 2.3), and EFAM (Section 2.4).

2.1. Additive manufacturing

AM is a manufacturing technology that builds 3D structures through digital, layer-by-layer fabrication. It has been widely applied in the fabrication of MNDs. However, due to material properties and process limitations, traditional AM still encounters challenges in material manipulation, microstructural control, and multifunctional integration. FAM enhances manufacturing precision and structural performance by introducing external physical fields to control material behavior during AM processes. Based on their forming mechanisms, FAM can be broadly categorized into nozzle-based AM and VPP-based AM. Nozzle-based AM relies on extrusion or jetting deposition of materials, making it suitable for high-viscosity materials and composite fabrication. In contrast, VPP-based AM utilizes photopolymerization reactions to construct fine structures, enabling high-resolution device manufacturing. To explore the application mechanisms of FAM in different AM technologies, this chapter elaborates on the principles of these two categories and their integration with external fields in Sections 2.1.1 and 2.1.2, respectively. The potential of each technology combined with field-assisted techniques is further evaluated in Table 1. Here, resolution is defined as the minimum manufacturable unit achievable by the device, distinct from precision discussed in subsequent sections, which refers to the consistency of outcomes across multiple repeated operations.

2.1.1. Nozzle-based additive manufacturing Nozzle-based AM is a class of AM technologies that rely on nozzle-based material deposition, primarily categorized into material extrusion (ME) and material jetting (MJ). These methods are widely applied in the fabrication of polymer composite materials and can be further optimized through field-assisted techniques to enhance deposition precision and functional properties. ME technology involves pushing or extruding materials via

a nozzle to form 3D structures layer-by-layer on a substrate. Its main subcategories include fused deposition modeling (FDM), direct ink writing (DIW), and inkjet printing. These technologies utilize thermoplastic polymers or nanocomposite materials as feedstocks, offering advantages such as low equipment costs and broad material compatibility. However, they are constrained by nozzle size and material rheological properties^[35,88,89]. For instance, DIW struggles with nozzle clogging when depositing high-viscosity composite inks due to limited nozzle diameters. The introduction of external fields, such as magnetic or acoustic fields, can mitigate clogging by improving material flow and enabling the printing of highly viscous materials^[90]. MJ technology selectively ejects liquid or semi-solid materials through nozzles onto a substrate, which are then solidified via curing. Its subcategories include aerosol jet printing, nanoparticle jetting, and EHDJ. MJ is renowned for high precision and multi-material printing capabilities. However, it faces challenges in droplet control and particle distribution^[91]. For example, aerosol jet printing often suffers from nanoparticle agglomeration during deposition, leading to uneven coatings. The incorporation of acoustic fields can effectively aggregate nanoparticles during printing, enhancing uniformity^[92,93].

2.1.2. Vat photopolymerization-based additive manufacturing VPP-based AM is a class of techniques that utilizes photocurable resins to form 3D structures via layer-by-layer photopolymerization. In vat processes, liquid photopolymer resins are polymerized under external light sources. The build platform sequentially lifts as each layer is cured, enabling the construction of complex geometries. This method achieves high precision and is suitable for micro- and nano-scale structures^[94–96]. Representative techniques include SLA, digital light processing (DLP), CLIP, TPP, and volumetric additive manufacturing (VAM)^[97]. These techniques rely on photochemical reactions, offering high precision and complex structure fabrication capabilities^[32]. Although these methods offer exceptional resolution and geometric freedom, they are still constrained by the limited variety of printable materials and insufficient mechanical properties of the prepared structures^[98]. For example, microstructures prepared via TPP often exhibit relatively poor mechanical properties^[99]. The introduction of acoustic fields enables instant patterning and assembly of nanoparticles within droplets, producing anisotropic polymer nanostructures with enhanced properties.

2.2. Magnetic field-assisted additive manufacturing (MFAM)

Magnetic fields, as an external field, offer unique advantages in AM, particularly in micro/nano-scale fabrication^[65,66]. Compared to electric or acoustic fields, magnetic fields provide rapid dynamic response, non-contact manipulation of materials, and precise spatial force adjustment, enabling high-precision control of micro/nanostructures. For instance, magnetic nanoparticles or ferromagnetic fillers can be aligned along sub-micrometer scales via Lorentz forces or magnetic

Table 1. Typical additive manufacturing technology and field-integrated evaluation.

	Moulding principle	Resolution	Advantages	Limitations	Integration potential
Fused deposition modelling (FDM)	Deposition of molten thermoplastic materials through nozzles	$>64 \mu\text{m}$ ^[76]	<ul style="list-style-type: none"> • Low-cost and widely available • Suitable for rapid prototyping 	<ul style="list-style-type: none"> • Low resolution. • Rough surface finish • Requires support structures 	Electric field-integrated: applies a high voltage to induce the formation of fine print lines via the electric field, the device resolution can be effectively improved ^[75]
Direct ink writing (DIW)	Extrusion of viscous liquids by pressure	$>50 \mu\text{m}$ ^[77]	<ul style="list-style-type: none"> • Handles complex materials • No need for support structures 	<ul style="list-style-type: none"> • Viscosity-dependent performance • Prone to nozzle clogging • Limited to slow printing speeds 	Magnetic field-integrated: aligns magnetic nanoparticles to break agglomerates and create aligned micro/nanostructures for anisotropic properties ^[59]
Material jetting (MJ)	Spraying photosensitive resins or adhesives onto substrates via droplet ejection	$>80 \text{ nm}$ ^[79]	<ul style="list-style-type: none"> • High precision • Multi-material printing capability • Minimal post-processing 	<ul style="list-style-type: none"> • Conductive path discontinuity • Limited to small-scale production • Material compatibility limits 	Electric field-integrated: aligns nanoparticles during droplet formation, creating continuous conductive paths for flexible sensors ^[78]
Stereolithography (SLA)	A laser scans and selectively polymerizes liquid photopolymer resin layer-by-layer using ultraviolet (UV) light, forming a solid structure	$>41.7 \mu\text{m}$ ^[80]	<ul style="list-style-type: none"> • Complex 3D microstructures 	<ul style="list-style-type: none"> • Material limitation • Surface roughness • Slow curing speed 	Magnetic field-integrated: aligns magnetic nanoparticles during curing to create anisotropic microstructures ^[80]
Digital light processing (DLP)	A digital micromirror device projects a pixelated UV light pattern onto the resin surface, curing an entire layer simultaneously	$>7.6 \mu\text{m}$ ^[82]	<ul style="list-style-type: none"> • Faster throughput • High resolution 	<ul style="list-style-type: none"> • Resin property dependency • Inter-layer adhesion 	Electric field-integrated: improves resin flow and inter-layer adhesion via electrostatic forces during curing ^[81]

(Continued.)

Table 1. (Continued.)

	Moulding principle	Resolution	Advantages	Limitations	Integration potential
Two-photon polymerization (TPP)	Near-infrared laser induces nonlinear absorption in a focal volume, enabling curing of resin at sub-micrometer/nanoscale resolution without thermal damage	$>35 \text{ nm}$ ^[55]	<ul style="list-style-type: none"> • Ultra-high resolution • 3D nanoscale architectures 	<ul style="list-style-type: none"> • High equipment cost • Slow printing speed 	Acoustic field-integrated: accelerated dispersion and assembly of nanoparticles ^[83]
Continuous liquid interface production (CLIP)	Resin is continuously cured at a moving liquid-solid interface through oxygen inhibition, eliminating layer-wise separation and enabling smooth surfaces	$>64 \text{ }\mu\text{m}$ ^[85]	<ul style="list-style-type: none"> • High-speed printing • Isotropic mechanical properties 	<ul style="list-style-type: none"> • Release film dependency • Layer thickness variability 	Magnetic field-integrated: guides magnetic nanoparticle alignment in continuous curing for anisotropic micro-channel arrays ^[84]
Volumetric additive manufacturing (VAM)	A volumetric laser projects a 3D light pattern into the resin, curing the entire structure simultaneously within the liquid bath	$>20 \text{ }\mu\text{m}$ ^[87]	<ul style="list-style-type: none"> • Single-step fabrication • Multi-functional features 	<ul style="list-style-type: none"> • Complex optical setups • Structural complexity limits 	Acoustic field-integrated: generates spatially varying pressure fields to guide resin polymerization and complex structure formation ^[86]

dipole reorientation, forming anisotropic conductive paths or programmable functional domains^[59,100]. This capability is critical for manufacturing MNDs such as magnetic-responsive actuators, where the precise orientation of particles directly determines performance^[88,101]. Magnetic fields possess inherent advantages, such as simultaneous material manipulation and structural programming. These capabilities make them indispensable for advanced AM applications demanding multi-functional integration.

The generation of magnetic fields in MFAM relies on two primary systems: permanent magnet systems and electromagnetic systems. Although permanent magnet systems are simple and cost-effective, they generate strong magnetic fields suitable for a broader range of high-field applications. However, the field strength and distribution generated by permanent magnets are limited, and precise control over the field strength is not possible. In contrast, electromagnetic systems can generate more uniform magnetic fields, with the ability to precisely adjust the magnetic field strength based on the current intensity^[102]. Electromagnetic systems, such as Helmholtz coils and multi-coil systems^[65], produce uniform fields and are particularly beneficial for applications requiring a uniform magnetization direction of ferromagnetic materials. The drawback of electromagnetic systems is their structural complexity, requiring additional control systems and cooling mechanisms.

In MFAM, materials that respond to magnetic fields are key to achieving precise control and high-performance fabrication. These materials include ferromagnetic materials, magnetic nanoparticles and shape-memory alloys^[103]. These materials can undergo structural changes or directional alignment under the influence of external magnetic fields, enabling precise directional shaping and enhanced functionality^[104]. By incorporating magnetic field control into AM, researchers can precisely regulate the alignment and structural optimization of materials, showcasing significant potential in high-end applications such as multi-material printing, functionally graded materials, and smart sensors and medical devices^[16,102,105]. In conclusion, the use of magnetic field-responsive materials offers greater design flexibility and performance optimization in AM.

MFAM offers distinct advantages in micro/nanoscale fabrication. The following sections categorize MFAM into two primary frameworks that align with AM techniques: nozzle-based systems (Section 2.2.1) and VPP-based systems (Section 2.2.2). A detailed analysis will be provided of representative MFAM systems, their manufacturing processes, and their associated advantages.

2.2.1. Nozzle-based MFAM. Permanent magnet actuation MFAM aligns magnetically responsive particles by positioning strong magnets near the nozzle, leveraging Lorentz forces or dipole interactions, and offers the key advantage of a stable static field without external power. This technique demonstrates significant potential in micro/nanoscale manufacturing, enabling precise modulation of microstructures through magneto-material interactions to enhance functional

integration. Kokkinis et al. developed a printing system integrating a single neodymium magnet beneath the nozzle, generating a magnetic field of approximately 200 mT (Figure 2(a))^[106]. The magnet offers two degrees of freedom (DOF), enabling control over particle orientation by adjusting the printed object's orientation relative to the magnet and the distance between the glass plate and the magnet. By coupling programmable materials with magnetic responsiveness, this system enables gradient-controlled magnetic programming during material curing. Neodymium-iron-boron (NdFeB) microparticles compounded with thermosetting resins align along the Z-axis under the applied magnetic field, forming gradient-magnetized layered structures suitable for functionally graded materials^[107]. Additionally, a ferromagnetic liquid crystal elastomer (magLCE) ink printing system driven by permanent magnets was proposed^[108], which uses a single permanent magnet with 3-DOF (Figure 2(b)). During printing, shear aligns nematic liquid crystal molecules in the magLCE ink, while the magnetic field reorients NdFeB particles, enabling tunable filament magnetization.

However, the limitations of single-magnet systems are increasingly evident: when printing complex 3D structures, the fixed spatial relationship between nozzle movement and the magnetic field may cause particle misalignment^[111,112]. For example, during curved-path printing in the XY plane, insufficient local magnetic field gradients may prevent complete particle alignment, reducing material anisotropy. To address this, a multi-magnet configuration (Figure 2(c)) has been proposed, where coordinated magnets generate an adjustable magnetic field direction^[73]. This system uses electromagnetic control to dynamically adjust magnet positions, enabling real-time alignment of the magnetic field with the nozzle trajectory. This approach allows multi-DOF manipulation: the magnetic field guides nozzle movement via force feedback, while particles dynamically align with the adjusted field during printing. However, spatial inhomogeneity in the magnetic field still causes localized misalignment. Notably, in high-viscosity ME, shear flow-magnetic field coupling delays particle alignment, ultimately reducing magnetically induced anisotropy in the cured structure^[65,113]. To further improve field uniformity, a ring-shaped permanent magnet design with a magnetic field intensity of 180 mT has been introduced^[114]. This design establishes a circumferential magnetic circuit around the nozzle, ensuring comprehensive field coverage. Its key innovation is optimizing magnetic field exposure by pre-aligning particles in a ring-shaped field before extrusion, ensuring precise alignment during deposition instead of relying on post-curing magnetization. This pre-alignment strategy significantly enhances the uniformity of magnetic filler distribution.

Electromagnet actuation MFAM offers greater flexibility and tunability compared to permanent magnet actuation MFAM. Electromagnetic systems allow for dynamic adjustment of magnetic field strength and direction by controlling the magnitude and polarity of electric current, enabling real-time alignment of magneto-responsive particles. This capability makes electromagnet actuation MFAM particularly

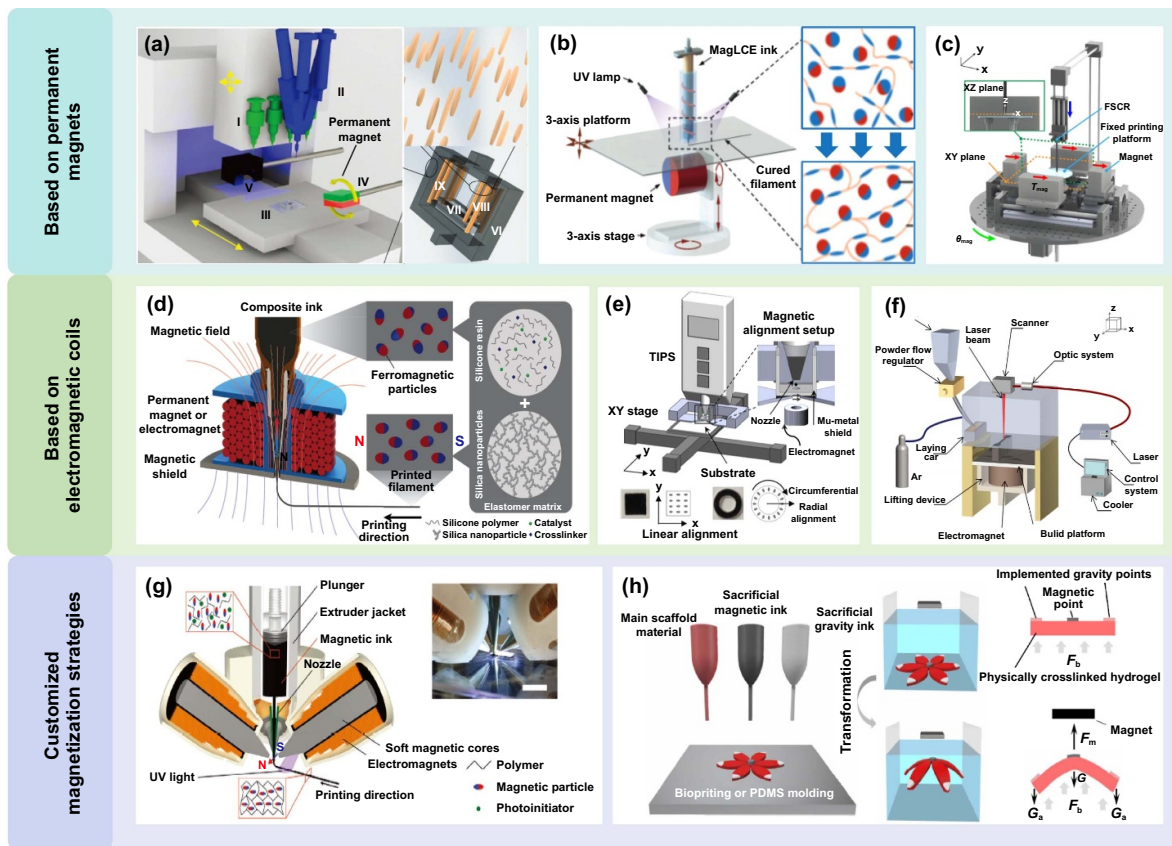


Figure 2. Magnetic field-assisted nozzle-based AM. (a) DIW printing device based on a single permanent magnet. Reproduced from^[106]. CC BY 4.0. (b) 3-DOF magLCE 3D printing system with a single permanent magnet. ^[108] John Wiley & Sons. © 2023 Wiley-VCH GmbH. (c) Example of a magnetically controlled printing system driven by multiple coordinated permanent magnets. Reproduced from^[73]. CC BY 4.0. (d) Example of using an electromagnetic coil to program magnetic particles during extrusion. Reproduced from^[59], with permission from Springer Nature. (e) Schematic of an inkjet printing and magnetic alignment setup based on an electromagnetic coil. Reprinted from^[109], with the permission of AIP Publishing. (f) Printing system for studying crystal orientation using alternating magnetic fields and static magnetostatic fields. Reprinted from^[110], Copyright (2022), with permission from Elsevier. (g) Example of an extrusion-based printing system assisted by three mutually orthogonal electromagnetic coils. Reproduced with permission from^[65]. CC BY-NC 4.0. (h) Printing strategy utilizing a magnetic field to induce 3D transformation in precursors after deposition. Reproduced from^[72]. CC BY 4.0.

advantageous for fabricating programmable magnetic materials, gradient magnetization structures, and complex magnetic domain patterns. Kim et al. introduced an electromagnetic actuation DIW method for printing soft materials with programmable ferromagnetic domains^[59]. The system integrates an adjustable electromagnetic coil surrounding the printing nozzle (Figure 2(d)), generating a 50 mT magnetic field to align NdFeB microparticles during extrusion. When using 20 vol% NdFeB particles, the printed magnetic structures achieve a magnetic moment density of $81 \text{ kA} \cdot \text{m}^{-1}$. Complex ferromagnetic domain programming is realized by adjusting the magnetic field direction. Electromagnetic devices for MFAM are typically located around the nozzle; however, particle aggregation may cause nozzle clogging during material programming. To address this issue, magnetic shielding devices made of high-permeability alloys can be installed around the nozzle.

To further study magnetically anisotropic device fabrication via magnetically actuated MFAM, an inkjet system integrated with electromagnetic control was proposed

(Figure 2(e))^[109]. This setup applies a 10 mT magnetic field beneath the inkjet nozzle, aligning cobalt-based nanoparticles along field lines during deposition. Aligned samples exhibited a 77% improvement in high-frequency permeability and reduced hysteresis losses compared to non-aligned counterparts. By adjusting the magnetic field direction and substrate motion, the method enables the fabrication of magnetic devices with diverse geometries. Zhou et al. investigated the effects of static and alternating magnetic fields on microstructure and mechanical properties^[110]. The experimental setup includes a cylindrical electromagnet beneath the printing platform, generating either a 300 Hz, 0.4 mT alternating magnetic field or a 19.71 mT static magnetic field, both aligned parallel to the build direction (Figure 2(f)). Interactions between induced currents and the magnetic field generate Lorentz forces in the melt pool. Results show that static fields suppress columnar grain epitaxial growth and alter crystal orientations, while alternating fields further refine microstructures and improve grain uniformity.

In MFAM, simple permanent magnets or a single electro-magnetic coil is commonly used to control the alignment and magnetization distribution of magneto-responsive particles. However, customized magnetic field strategies can also be used to manipulate the arrangement of magnetic particles. In this review, customized magnetization strategies include two main aspects: (i) using a multi-axis electromagnetic coil system or a system that combines permanent magnets with electromagnetic coils to achieve an approximately uniform magnetic field or multi-degree-of-freedom control of the magnetic field during the printing process. (ii) optimizing the manufacturing process or magnetization approach so that, after printing, a magnetic field can be applied to alter the uncured structures or to program the magnetic domains of the device. Unlike the previously mentioned methods, where the magnetic field is applied during printing, applying the magnetic field after printing to program the magnetic domains can also be considered a form of MFAM. From a manufacturing perspective, changing the magnetic domains with a magnetic field is still part of the fabrication process. Therefore, this review classifies such processes of post-printing magnetization under the category of MFAM. Customized magnetization strategies enable more flexible magnetic field control. They help create complex and multifunctional magnetic materials and devices.

A three-axis electromagnetic coil system was used as the magnetic field generator in MFAM (Figure 2(g))^[65]. This system consists of three mutually orthogonal electromagnetic coils symmetrically surrounding the extrusion nozzle, with each coil forming an angle of 54.74° with the nozzle. The net magnetic field generated by this system can be oriented in any direction, providing 3-DOF for particle alignment, and enabling the fabrication of soft robots with complex magnetization patterns such as helices and sine waves. Similar three-coil designs have also been adopted in printing systems capable of achieving multiple fiber orientations^[115].

Carefully designed printing processes and magnetization strategies can similarly produce magnetic devices such as vascular stents and soft magnetic actuators. It is worth noting that, in addition to applying magnetic fields during the printing process, MFAM strategies also include scenarios where field manipulation can be carried out after printing to further control or program material properties. Xie et al. proposed a 3D printing method based on magneto-responsive hydrogels, where the magnetic field primarily influences the post-print manipulation stage rather than the printing process itself^[72]. The research team first prepared flat hydrogel precursors containing multiple inks during the printing process. After 3D printing, the precursors were immersed in a water bath, and a single permanent magnet was used to apply a magnetic field. Under the combined effects of magnetic force, gravity, and buoyancy, the flat precursors transformed into 3D structures (Figure 2(h)). This case demonstrates how the application of external magnetic fields after printing can be used to alter and reconfigure as-printed structures. This method enables programmable post-printing shape transformation, thereby expanding the design freedom and multifunctionality of fabricated devices. It is noteworthy that the magnetic

fields used to induce such post-printing deformation are not strictly limited to NdFeB magnets, as these magnets can only produce gradient magnetic fields^[16]. Systems such as circular or saddle-shaped coil arrangements and eight-coil configurations are capable of generating spatially uniform magnetic fields, which may also facilitate similar shape morphing after printing^[116,117]. This integration strategy provides greater design freedom, enabling the fabrication of complex, reconfigurable and multifunctional magnetic structures.

2.2.2. Vat photopolymerization-based MFAM VPP-based MFAM differs significantly from nozzle-based approaches. In nozzle-based systems, magnetic fields are typically applied around the nozzle to control the orientation of magnetic particles either before or during ME^[34]. In contrast, VPP-based MFAM applies magnetic fields around the resin vat, where the alignment of magnetic particles is directly determined by the direction of the magnetic field. This eliminates the need to account for post-extrusion directional changes or the influence of nozzle-induced shear forces on particle orientation^[65], which are common challenges in nozzle-based systems. Consequently, VPP-based MFAM demonstrates broader applicability and holds significant potential for advanced manufacturing applications. Permanent magnet actuation VPP-based MFAM uses a static magnetic field during printing to guide magnetic fillers along field lines. This enhances the composite's anisotropy, magnetic responsiveness, and mechanical properties. This approach is particularly suitable for applications requiring pre-defined magnetization directions, such as shape-programmable structures and magnetically actuated microrobots.

Figure 3(a) illustrates a DLP-based permanent magnet-assisted photocuring system^[66]. The substrate material is prepared by mixing pre-magnetized hard magnetic particles with flexible UV resin. A single cuboidal permanent magnet is arranged around the printing substrate. After the particles within the substrate are reoriented by the magnetic field, a DLP projector emits ultraviolet light in selected regions of the substrate, initiating polymerization and freezing the alignment of magnetic particles in these regions. Repeating this process encodes localized magnetization directions into the planar material, enabling the creation of programmable structures. Lu et al. developed a magnetic field-assisted projection SLA process, which also utilizes a single permanent magnet. By controlling the rotation of the magnetic field and the distance between the magnet and the resin vat, this process effectively manipulates the dispersion or alignment of magnetic particles^[80]. Three test cases—impellers, dual-wheel rollers, and flexible films—were fabricated to verify the feasibility and effectiveness of the process. Additionally, this technique can be applied to medical microneedles. By aligning iron oxide nanoparticles into bundles, it enables the fabrication of microneedle arrays with a biomimetic limpet tooth-like layered structure^[118].

To further explore permanent magnet actuation MFAM, Wu et al. developed a DLP-based 4D printing technology that

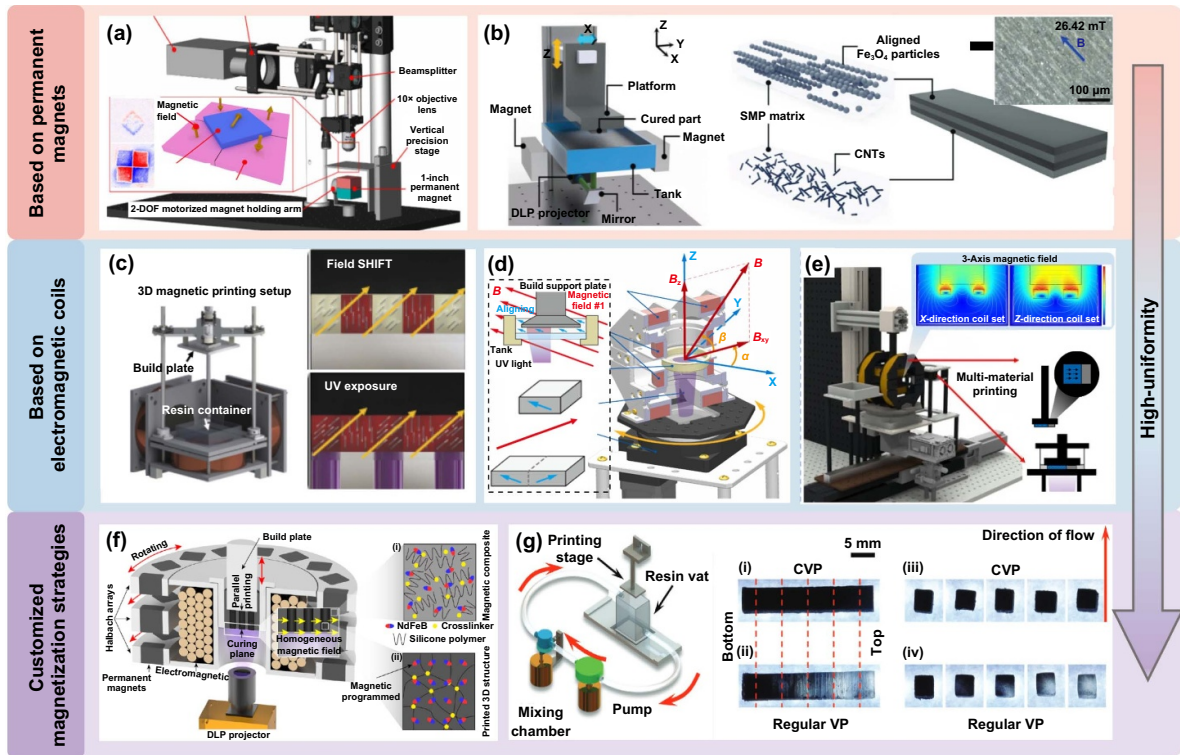


Figure 3. Magnetic field-assisted VPP-based AM. (a) Single permanent magnet-based particle patterning device. From^[66]. Reprinted with permission from AAAS. (b) Dual permanent magnet DLP 3D printing system. ^[119] John Wiley & Sons. © 2024 Wiley-VCH GmbH. (c) Voxel-based magnetic photopolymerization 3D printer setup. Reproduced from^[120]. CC BY 4.0. (d) 2-DOF Helmholtz coil-assisted DLP printing system. Reprinted from^[67], Copyright (2024), with permission from Elsevier. (e) Multi-material DLP printing system with a horizontal liquid exchange mechanism. Reproduced from^[121], with permission from Springer Nature. (f) Printing system assisted by an integrated Halbach array and electromagnetic coils. Reproduced from^[100]. CC BY 4.0. (g) CVP printing device. ^[122] John Wiley & Sons. © 2022 Wiley-VCH GmbH.

integrates the directional alignment of magneto-responsive particles with alternating high-conductivity layers to achieve multi-modal actuation. The research team employed two N52 NdFeB permanent magnets (64 mm × 54 mm × 36 mm, magnetic field strength (25 ± 0.5) mT) to provide a nearly uniform magnetic field during the DLP printing process, ensuring Fe₃O₄ particle alignment along the magnetic field lines^[119]. During printing, two resin vats were prepared for alternation, enabling the fabrication of devices with alternating conductive layers (Figure 3(b)). It is evident that VPP-based MFAM eliminates concerns related to nozzle-based systems, such as direction conversion, magnetic particle agglomeration, and magnetic shielding^[102,123,124]. However, the fixed magnetic field direction and strength provided by permanent magnets are insufficient to further advance VPP-based MFAM for fabricating MNDs with superior magnetic properties.

Electromagnet actuation VPP-based MFAM enables more complex magnetic structure programming. Martin et al. developed an electromagnetic-assisted SLA printing method for fabricating high-strength bioinspired composite materials. The key innovation of this study lies in utilizing magnetic labeling techniques to enable precise alignment of traditionally non-magnetic reinforcement particles under an applied magnetic field. The experimental setup employed electromagnetic coils with adjustable field strength, where

each printed layer was first subjected to a magnetic field to align the particles in a predefined direction, followed by DLP for photocuring, resulting in programmable reinforcement architectures (Figure 3(c)).^[120] Compared to permanent magnet systems, electromagnetic systems are better suited for printing programmable structures, and the uniformity of the electromagnetic field is one of the critical factors for printing high-performance devices. The integration of VPP technology with a 2-DOF Helmholtz coil system enables the fabrication of flexible actuators with specialized groove structures. The printing system (Figure 3(d)) generates uniform magnetic fields in the X and Z directions only^[67]. The DLP setup is located at the bottom of the device, and the coil section is rotatable. By determining angles α and β, a magnetic field in any direction can be generated. Under a uniform magnetic field, the curing pattern can be divided into different regions for sequential curing. Before each exposure, an alignment magnetic field is applied. Each ‘alignment-curing’ process produces a region with a unique magnetization orientation. The constructed groove structures enhance actuator deformation, effectively addressing the issue of insufficient driving force caused by low magnetic particle content.

While there have been numerous studies on single-material MFAM, the range of devices that can be printed using single materials is limited. Therefore, exploring multi-material

MFAM has become a key focus of current research^[62,103,125]. A multi-material MFAM technique incorporating a uniform magnetic field has been proposed. This method is also based on DLP technology, using Helmholtz coils as the magnetic field generator, and innovatively integrates a horizontal liquid exchange system. Embedded within the resin vat, the system includes a 3D auxiliary magnetic field generator, a conventional vat seat, and a cleaning mechanism. The cleaning mechanism allows seamless switching between the three manufacturing positions via a horizontal translation mechanism (Figure 3(e)). During multi-material printing, the horizontal liquid exchange system is primarily used. After the magnetic slurry structure is printed, the resin vat is cleaned and replaced to continue printing the flexible structure. Experimental studies have shown that this technique enhances the mechanical stability and magnetic responsiveness of heterogeneous composite structures, making it particularly suitable for fabricating smart materials and tunable magnetic devices^[121].

In VPP-based MFAM, the uniformity of the magnetic field and the alignment of magnetic particles significantly impact the final structural properties. In addition to Helmholtz coils, circular and saddle-shaped arrays of permanent magnets^[100,114,117], as well as Halbach arrays, are commonly used to generate uniform magnetic fields. By integrating a Halbach array with an electromagnetic solenoid (Figure 3(f)), a high-density and uniform magnetic field can be generated. This approach optimizes the alignment of magnetic particles before photocuring, reducing filler aggregation and thereby improving both magnetization precision and structural uniformity. Additionally, the research team introduced a support strategy involving localized reinforcement and spacing optimization to further enhance printing stability. For fabricating devices with uniform magnetization, a uniform magnetic field is one critical factor, while another important factor is the dispersion of magnetic particles within the resin. In traditional VPP printing, particles in the resin tend to settle quickly, potentially leading to uneven particle distribution within the printed material^[126]. Combining circulating VPP 3D printing technology addresses this issue effectively. This method utilizes a resin circulation system to prevent particle sedimentation and incorporates bifurcating fluidic manifolds to ensure uniformity in large-scale prints. The study employed $\text{SrFe}_{12}\text{O}_{19}$ magnetic particles, chosen for their low UV absorbance and strong magnetic response, allowing a high loading ratio of up to 30% while maintaining uniform dispersion. After printing, the devices were subjected to magnetic programming in a 9-coil system. The circulating vat photopolymerization (CVP) method effectively improved the magnetic particle loading rate and magnetic responsiveness of the devices (Figure 3(g))^[122].

MFAM enhances precision and functional integration in micro/nanoscale fabrication through dynamic interactions between magnetic fields and magnetic materials. Its core value lies in integrating the regulation of material microstructures with macroscopic functional programming. Technically, nozzle-based systems use real-time magnetic fields to dynamically align particles during extrusion. They offer fast responsiveness but face limitations from particle

migration delays in high-viscosity materials and challenges in achieving uniform magnetic fields. In contrast, photopolymerization systems fix the orientation of magnetic fillers in the resin vat under a uniform magnetic field, avoiding nozzle-induced shear effects. However, they still require optimization for multi-material compatibility and dynamic magnetic field control. The breakthrough of MFAM is reflected in its ability to impart variable magnetic responses, mechanical anisotropy, and smart deformation capabilities to materials through magnetic programming. This advancement shifts the manufacturing paradigm from passive deposition to active field-driven 'structure-function' co-design, providing efficient solutions for multifunctional devices in fields such as soft robotics and medical implants.

2.3. Acoustic field-assisted additive manufacturing (AFAM)

While MFAM leverages the unique interactions between magnetic fields and responsive materials to achieve precise micro/nanoscale control, other external fields, such as acoustic fields, offer alternative mechanisms for material manipulation, expanding the toolbox for advanced AM. AFAM demonstrates unique advantages in micro/nanoscale fabrication. The key distinction between acoustic fields and magnetic fields lies in their operating principles. Magnetic field effects typically rely on the magnetic responsiveness of materials, often necessitating the pre-magnetization of printing materials or resins^[102,103]. In contrast, acoustic fields directly act on materials through mechanical wave effects, without depending on the material's conductivity or magnetic properties, thus providing broader material compatibility^[58,127,128]. This makes acoustic fields particularly suitable for manipulating non-magnetic or low-conductivity materials^[129,130]. By precisely adjusting the frequency, intensity, and direction of sound waves, pressure gradients or standing wave fields can be generated to drive particle migration, droplet directional ejection, or nanostructure self-assembly, achieving micron-scale spatial control^[34,93]. For example, Surface Bulk Acoustic Waves (SBAW) can guide cells within the printing vat to construct biomimetic implants such as menisci^[131–133]. Additionally, by dynamically adjusting the positions of standing wave nodes, acoustic fields enable real-time reorganization of material distribution, facilitating the construction of conductive microstructures^[134].

In AFAM, the primary action of acoustic fields occurs through acoustic radiation force, which generates pressure gradients via sound waves. These gradients create forces acting on suspended materials, causing fluids and solid materials with different densities to move toward pressure nodes or antinodes^[135]. Printing based on acoustic radiation force can be categorized into two types: focused acoustic fields and sound wave-guided self-assembly. The former involves acoustic devices, such as focusing transducers or acoustic lenses, generating focused acoustic beams that act like tweezers to capture and manipulate materials or individual droplets. The latter relies on carefully arranged transducers and mirrors to produce various acoustic fields with multiple pressure nodes, driving materials and particles to move toward

these nodes and form desired microstructures and patterns. By changing the frequency and direction of sound waves, this method allows flexible control over the spatial distribution of materials. In sound wave-guided self-assembly, the acoustic field can be roughly divided into unidirectional, multidirectional, and omnidirectional fields based on the arrangement of transducers, with spatial control enhanced from single-path to full-domain manipulation. Additionally, in AFAM, besides using acoustic radiation force to regulate material printing, special acoustic effects such as acoustic cavitation and acoustic thermal effects can also be utilized for auxiliary printing.

The following sections categorize AFAM into two primary frameworks that align with AM techniques: nozzle-based systems (Section 2.3.1) and VPP-based systems (Section 2.3.2). A detailed analysis will be provided of representative AFAM systems, their manufacturing processes, and their associated advantages.

2.3.1. Nozzle-based AFAM. In nozzle-based AFAM, the integration of acoustic fields provides a new means of controlling material flow, distribution, and alignment. Through focused acoustic fields or acoustic field-guided self-assembly, sound waves not only influence the material flow around the nozzle but also enable the orderly arrangement of materials and particles after printing. Compared to traditional nozzle-based AM techniques, the integration of acoustic fields effectively improves material uniformity, prevents particle aggregation, and enhances printing precision. Additionally, acoustic radiation forces can precisely regulate droplet morphology, size, ejection direction, and speed, ensuring stability and uniformity of droplets during the printing process.

Chansoria et al. described a biofabrication method driven by bulk acoustic wave ultrasound. The method utilizes a set of transducers and reflectors to generate acoustic waves that align cells and particles within GelMA hydrogels at pressure nodes in the plane, enabling the fabrication of heterogeneous tissues (Figure 4(a))^[131]. The study demonstrated that adjusting the ultrasound frequency and intensity allowed precise control over the self-assembly of cells, collagen microaggregates, and polycaprolactone microfibers, promoting orderly cell arrangement and improving the microstructure and mechanical properties of the biofabricated material. This method enables precise control of cell patterns for tissue engineering applications, fabricating tissue constructs with natural organizational structures. Similarly, the work using single piezoelectric transducers to generate acoustic fields for guiding particle self-assembly has also demonstrated this point^[133,136]. In addition to using acoustic fields to align materials after extrusion, pre-extrusion alignment is also a method for fabricating microstructures. By arranging two piezoelectric plates around the nozzle and placing the nozzle between them, the material inside the nozzle is influenced by the acoustic field before printing. Adjusting the distance between the piezoelectric plates modifies the wavelength of the acoustic waves in the field, thereby altering the alignment and spacing of fibers within the material (Figure 4(b)). This

adjustment influences the material's electrical and mechanical properties. This method enables the fabrication of flexible bioinspired materials with customizable properties, showcasing the immense potential of using ultrasound to precisely control material self-assembly^[137].

Acoustic focusing utilizes the focusing effect of sound waves to precisely position droplets or particles, thereby aiding in the ordered arrangement of materials. Liu et al. investigated the application of AFAM in carbon fiber-reinforced polydimethylsiloxane (PDMS) composites. The printing system encompasses three parts: AF generation, printing, and AF monitoring (Figure 4(c))^[138]. In the AF generation system, a waveform generator produces high-frequency sine waves, which are amplitude-controlled via an amplifier to excite annular piezoelectric ceramics, providing an in-situ acoustic field. In this setup, the annular piezoelectric ceramic generates a focused acoustic field around the extrusion nozzle, which improves material quality by influencing material flow and consolidation processes. The study demonstrated that introducing an acoustic field effectively reduced internal defects such as air bubbles and uneven distribution in the printed material. The incorporation of the acoustic field not only improved the microstructure of the material but also significantly enhanced the tensile properties of the composite, particularly in terms of elongation and toughness. Additionally, an enhanced aerosol jet printing method utilizing annular acoustic focusing was explored. By introducing an optimal focusing frequency of 5.8 MHz, the acoustic field further reduced the diameter of the ink flow during printing and allowed precise control over the deposited linewidth through acoustic field modulation (Figure 4(d)). Experimental results showed that this method reduced the linewidth by 60% while increasing the conductivity of the printed device by 180%^[93].

Focused acoustic fields can also act before the extrusion process of printing materials. When the acoustic pressure focal point is located at the air-liquid interface, the kinetic energy flow generated by the acoustic pressure overcomes the liquid's interfacial energy. According to Rayleigh-Taylor instability, a certain amount of liquid is ejected at the focal point, forming droplets. Additionally, by controlling the pressure gradient of sound waves, the movement direction of droplets can be manipulated, allowing them to deposit onto the printing substrate, forming unique printed structures. This novel droplet printing method uses an acoustic field to achieve high-resolution, precisely controlled droplet printing, capable of generating single droplets in the air. Under different acoustic wave penetration forces and nozzle diameters (d), the size of the formed droplets varies (Figure 4(e))^[139]. Extruded materials are often affected by nozzle shear forces, which can significantly impact cell viability. To address the challenges of cell printing, especially with high cell concentrations, a nozzle-free printing system was proposed (Figure 4(f)). The study demonstrated that compared to a microvalve nozzle with a diameter of 150 μm , the maximum shear stress during the nozzle-free printing process was reduced by 2.7 times^[74]. The nozzle-free system enables the precise ejection of high-concentration cells and other bioinks to predefined locations

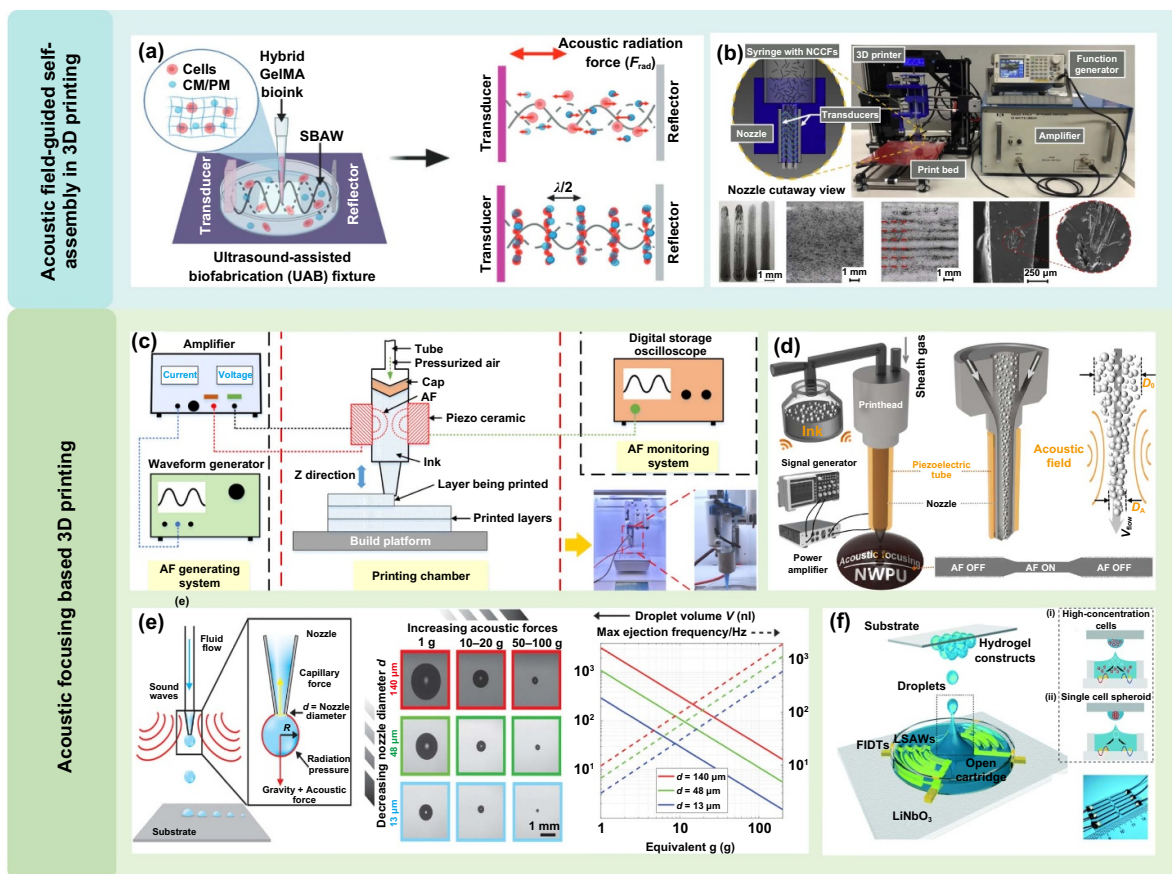


Figure 4. Acoustic field-assisted nozzle-based AM. (a) Schematic of SSAW printing and particle manipulation. Reproduced with permission from^[131]. CC BY-NC-ND 4.0. (b) Ultrasound-assisted printing device with pre-extrusion alignment. Reprinted from^[137], Copyright (2020), with permission from Elsevier. (c) Acoustic field system for printing carbon fiber-reinforced PDMS composites. Reprinted from^[138], Copyright (2022), with permission from Elsevier. (d) Aerosol jet printing enhanced by annular acoustic fields. Reproduced from^[93], with permission from Springer Nature. (e) Acoustically induced droplet jet printing and droplet size variations with different diameters. From^[139]. Reprinted with permission from AAAS. (f) Nozzle-free printing system for high-concentration cell printing. Adapted from^[140] with permission from the Royal Society of Chemistry.

while maintaining high cell viability (>94%)^[140]. This technology offers new perspectives for precise cell positioning and the fabrication of complex cellular structures. Focused acoustic fields significantly enhance extrusion-based AM by improving material quality and deposition precision, with applications evolving from nozzle-assisted to nozzle-free systems. This progression is particularly impactful for bioprinting, where nozzle-free acoustic focusing enables the gentle and precise ejection of high-concentration cells, thereby preserving high cell viability.

2.3.2. Vat photopolymerization-based AFAM. In VPP-based AFAM, acoustic field-guided self-assembly enables precise control over particle alignment within photocurable resins. The key to this approach lies in transducer placement, where different numbers and orientations of transducers generate diverse acoustic field patterns, influencing microscale material organization. For instance, opposing transducers generate unidirectional standing waves to achieve linear

particle alignment, while configurations with four to eight transducers create omnidirectional fields in a plane, enabling uniform alignment in multiple directions^[63,135,141,142]. Additionally, rotating transducers combined with ultrasonic vibrations enhance dynamic particle manipulation within the photocurable medium^[143,144]. Some studies employ specialized transducers or voxel-level acoustic field control, further improving material alignment precision during photocuring^[86].

An ultrasonic-assisted light-curing 3D printing method is proposed, which employs two opposing transducers to generate a stable standing wave field in the resin bath to guide the directional alignment of the enhancement particles during the curing process. By controlling the frequency and intensity of the acoustic field, this method enables dynamic adjustment of particle orientation, ensuring uniform distribution throughout the printing process (Figure 5(a))^[145]. To further increase the number of transducers, an ultrasound-assisted light-curing 3D printing system is proposed, which employs four symmetrically arranged transducers to achieve

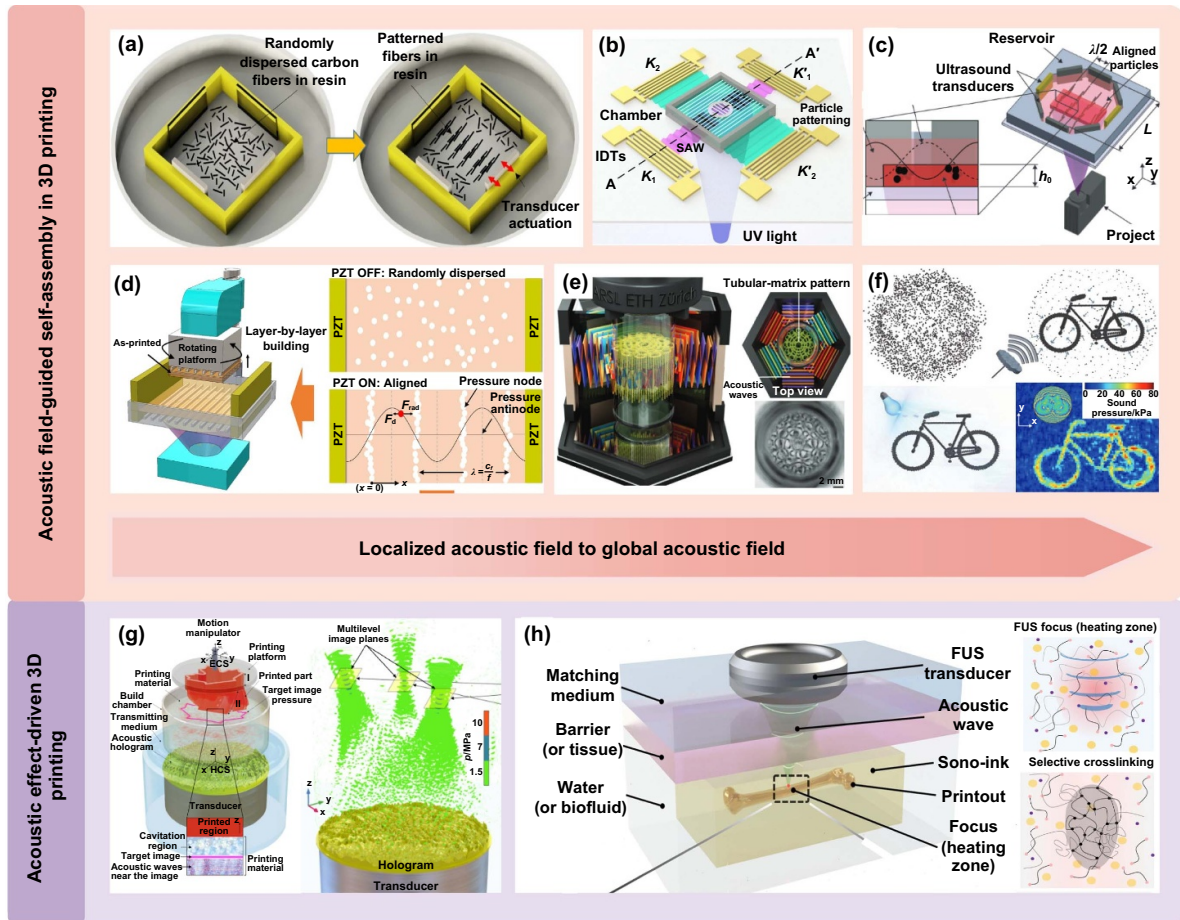


Figure 5. Acoustic field-assisted VPP-based AM. (a) Acoustic array system with two opposing transducers. Reprinted from^[145], Copyright (2020), with permission from Elsevier. (b) Ultrasonic-assisted photopolymerization 3D printing system featuring four symmetrically arranged transducers. Reprinted from^[146], Copyright (2024), with permission from Elsevier. (c) Printing system with eight interdigital transducers.^[135] John Wiley & Sons. © 2017 WILEY-VCH Verlag GmbH & Co. KGaA, Weinheim. (d) Printing system integrating ultrasonic fields with a rotating build platform. Reprinted from^[143], Copyright (2022), with permission from Elsevier. (e) Voxel-level volumetric 3D printing system with a global acoustic field. Reproduced with permission from^[86]. CC BY-NC 4.0. (f) The overall process of sound holographic field-assisted manufacturing.^[147] John Wiley & Sons. © 2017 WILEY-VCH Verlag GmbH & Co. KGaA, Weinheim. (g) 3D printing system leveraging acoustic cavitation effects. Reproduced from^[148]. CC BY 4.0. (h) Deep-penetration acoustic volumetric printing systems. From^[149]. Reprinted with permission from AAAS.

multidirectional homogeneous alignment of particles in the resin bath. This strategy ensures a homogeneous distribution of reinforcing particles in printed structures, improving the anisotropic mechanical properties of composites. Furthermore, the study investigates the effects of frequency combinations on particle self-assembly behavior, providing theoretical guidance for optimizing acoustic field parameters (Figure 5(b))^[146]. Building on the concept of using multiple transducers to create controlled acoustic fields, systems with an even greater number of transducers have been developed to enable more versatile particle patterning. For example, one such system utilizes an octagonal reservoir lined with eight ultrasound transducers around its perimeter (Figure 5(c))^[135]. This configuration allows for the precise computation of transducer settings to assemble a wide variety of particle patterns within a liquid photopolymer resin, with particles typically accumulating at the pressure nodes of the generated standing wave field. In one demonstration, by energizing two

opposing transducers within this eight-transducer array, parallel lines of particles were formed at the nodes of the resulting standing wave field, spaced a half-wavelength apart. This patterned resin is then selectively cured layer-by-layer using a DLP projector, effectively fixating the particle arrangement. Such an approach facilitates the layer-by-layer fabrication of engineered materials with user-specified microstructures, offering enhanced control over the material’s mesoscale architecture. Compared to systems with two or four transducers that typically generate simpler linear or grid patterns, an eight-transducer array, by enabling the computation of complex transducer settings, can theoretically generate a much wider range of user-defined particle patterns. This enhanced patterning capability significantly increases the design flexibility within VPP-based AFAM.

In order to further increase the freedom of the sound field, Li et al. proposed a photocuring AM method integrating an ultrasound field with a rotating build platform. An ultrasonic

transducer array applies a controllable acoustic field to the photopolymer resin, while the rotation of the platform allows particles on the printing platform to be subjected to the acoustic field in different directions. By combining the rotating platform with adjustments to the acoustic wave frequency and phase, the acoustic field can guide particle arrangement to form anisotropic structures (Figure 5(d))^[143]. The integration of the rotating platform eliminates the limitations on particle arrangement imposed by the number and distribution of transducers, further expanding the range of acoustic patterns that can be printed using AFAM. Beyond fixed configurations or platform rotation, dynamic pattern control is also achieved by actively changing the relative position between the sample and the acoustic source. A hexagonal setup with six piezoelectric transducers creates standing waves, guiding particle assembly into patterns like tubular matrices (Figure 5(e))^[86]. Crucially, translating the sample container dynamically alters the acoustic field patterns, enabling diverse and reconfigurable arrangements. Unlike computationally controlled static patterns from many transducers, this approach leverages simple physical movement for dynamic, real-time pattern adjustments, increasing AFAM flexibility.

As the demand for generating highly complex and arbitrary acoustic field patterns continues to grow, acoustic holography has emerged as a powerful technique for achieving global acoustic fields. This method utilizes computational acoustic holograms to precisely modulate the input ultrasound generated by transducers. As the ultrasound passes through the hologram, the wavefront is shaped according to the hologram's design, forming a pre-encoded 3D holographic sound field within the printing area through diffraction and interference. By exposing particles arranged along the holographic sound pressure field to ultraviolet light, corresponding structural devices can be fabricated, forming a pre-encoded 3D holographic sound field within the printing area through diffraction and interference. By exposing particles arranged along the holographic sound pressure field to ultraviolet light, corresponding structural devices can be fabricated (Figure 5(f))^[147]. The key advantage of acoustic holography lies in its ability to directly assemble particles in a suspension into almost any arbitrary shape without contact or masks, and independently of container geometry, providing unprecedented flexibility for micro-scale structural design in AFAM.

In VPP-based AFAM, in addition to utilizing acoustic radiation forces generated by acoustic fields to regulate printing materials, acoustic effects such as acoustic cavitation, acoustic streaming, and acoustic thermal effects can also be employed to influence photopolymerization and microstructural formation. Focused ultrasound-induced acoustic cavitation effects trigger sonochemical reactions in highly localized cavitation zones, enabling material curing and deposition for 3D printing. Building upon this principle, holographic direct sound printing (HDSP) utilizes acoustic holograms to pattern acoustic waves and induce regional polymerization simultaneously across a cross-section, moving beyond the voxel-by-voxel approach (Figure 5(g))^[148]. Through extensive experimental observations and material property analysis, researchers conducted

in-depth studies on the process parameters, material properties, and printing resolution of HDSP. These studies indicate that by adjusting the duty cycle, this method can print complex structures with controllable porosity and transparency. Furthermore, a self-enhancing sono-ink has been proposed, leveraging ultrasound penetration and acoustic thermal effects to significantly improve the curing depth of photopolymer resins. By incorporating ultrasound-absorbing nanoparticles into the resin, this method achieves localized heating, reduces the photopolymerization threshold, and enables deep-penetration volumetric printing (Figure 5(h))^[149]. Experimental results demonstrate that this approach allows for deeper curing under low-intensity light exposure while enhancing uniformity and resolution, paving the way for applications of photopolymer-based AFAM in biomedicine, optical devices, and microelectromechanical systems.

AFAM leverages the mechanical wave interactions between sound waves and materials to overcome limitations in micro/nano-scale structural control and material compatibility inherent to conventional manufacturing. Its core innovation lies in non-contact precision manipulation through two mechanisms: acoustic radiation forces and sound wave-guided self-assembly. Acoustic radiation forces directly regulate material flow and particle distribution via pressure gradients—for instance, stabilizing liquid metal droplet morphology or suppressing agglomeration in composite materials. Meanwhile, sound wave-guided self-assembly induces spontaneous material organization by adjusting frequency and direction, such as ultrasound-directed alignment of carbon fibers to customize mechanical properties or surface acoustic wave manipulation of nanoparticles for microfluidic device fabrication. AFAM's key advantage resides in its universality and multifunctionality: it operates independently of material electrical conductivity or magnetic responsiveness, accommodating non-magnetic or low-conductive materials. By programming acoustic fields, it synchronously controls material microstructure and macroscopic functionality, driving a paradigm shift toward 'field-driven structure-function co-design'. Technically, nozzle-based systems optimize droplet precision and material homogeneity through radiative forces. The VPP-based system integrates acoustic focusing and self-assembly for microscale programming. Future advancements require overcoming challenges in acoustic field uniformity, multi-field synchronization, and dispersion stability of high-concentration suspensions to unlock AFAM's potential in flexible electronics, biomimetic organs, and smart sensing technologies.

2.4. Electric field-assisted additive manufacturing (EFAM)

The electric field, a physical phenomenon generated by electric charge or current, is an important mechanical effect widely used in various material processing and particle manipulation applications. Its core properties include the strength, direction, and polarity of the electric field, which can be utilized to control charged materials or particles^[64]. Unlike magnetic fields, the application of electric fields in AM relies on the presence

of a medium^[102]. Magnetic fields directly interact with materials through magnetic forces without requiring a medium, acting on any magnetizable substance. In contrast, electric fields depend on the electrical conductivity of the medium to transmit forces via charges or ions within it. This medium dependency allows electric fields to be applied to a broader range of materials, including non-conductive ones, by introducing electrolyte solutions or charged particles into the medium^[150,151]. However, it also imposes constraints, as effective manipulation of non-conductive materials necessitates the presence of ions or charged species.

Electric fields are extensively applied in modern manufacturing, particularly in material processing, microstructural fabrication, and functional surface treatments^[152–154]. By applying electric fields, manufacturers can precisely manipulate particle movement, enabling uniform deposition, directional alignment, and surface modification processes. In thin-film and coating fabrication, electric fields are widely used in electrodeposition, where field strength and distribution control the deposition of metal ions or other materials onto substrates, forming high-quality coatings^[150]. Additionally, electric fields are employed in microstructural control of materials, such as guiding particle alignment to enhance material properties or using electrophoretic deposition (EPD) to achieve uniform distribution^[155]. In plastic and composite molding, electric fields help control the orientation of fillers or fibers, optimizing the material's mechanical properties and conductivity. Electric fields also play a crucial role in micro/nano fabrication, where they manipulate small particles by adjusting field strength and direction, facilitating the production of precise microsensors, microfluidic devices, and nanomaterials^[156–159]. Furthermore, electric fields are used in biomedical material manufacturing, guiding the directional alignment and growth of cells, and providing new technological support for tissue engineering and bioinspired material fabrication^[160].

Electric fields have been widely applied in numerous studies related to AM, particularly in material deposition, particle alignment, and microstructural optimization. One prominent technique is EHDJ, which uses a strong electric field applied between a nozzle and a substrate to overcome liquid material's surface tension. This field induces charge accumulation at the liquid meniscus, deforming it into a conical shape known as a Taylor cone, from which a fine jet or individual droplets are ejected due to Coulombic forces. The formation of this stable Taylor cone is critical for controlled material ejection. This allows for precise control over droplet volume, ejection frequency, and deposition accuracy, making EHDJ essential for achieving micron-level or even sub-micron resolution printing of various materials in microelectronics, biomedical scaffolds, and sensors^[161]. Additionally, EPD utilizes DC electric fields to drive charged particles suspended in a colloidal solution towards an oppositely charged electrode, enabling their uniform deposition to form high-quality coatings or 3D structures. By controlling field strength and particle characteristics, EPD ensures material uniformity, structural stability, and enhances interlayer bonding and functionality across a wide range of materials like ceramics, polymers, and metals. Furthermore,

electric fields are applied in the fabrication of self-assembling materials, guiding the alignment of particles or nanomaterials to form functional microstructures^[162]. Another notable method is electric poling-assisted additive manufacturing (EPAM), which utilizes electric fields to redistribute internal charges within materials, inducing polarization and altering their physical and chemical properties during the manufacturing process. For instance, this method can influence material viscosity, surface tension, and crystal growth direction^[163].

The following sections categorize EFAM into two primary frameworks that align with AM techniques: nozzle-based systems (Section 2.4.1) and VPP-based systems (Section 2.4.2). A detailed analysis will be provided on representative EFAM systems, their manufacturing processes, and their associated advantages.

2.4.1. Nozzle-based EFAM. The integration of electric fields with nozzle-based AM provides a precise method for material control. A typical example of this combination is electrospinning, which applies a high voltage between the nozzle and the substrate, and the Coulomb force exerted by the electric field on conductive materials forms a Taylor cone. Under the influence of this electric field, the polymer solution is stretched from the Taylor cone into a stable jet stream (Figure 6(a))^[164]. To explore the resolution of electrospinning technology, Melt Electrospinning Writing has been developed. This technique integrates electrostatic processes with direct writing and enables ultrafine fiber deposition by precisely controlling parameters such as polymer melt flow rate, nozzle diameter, applied voltage, and collector distance (Figure 6(b)). The method achieves direct writing of submicron fibers, with an average fiber diameter of $(817 \pm 165) \text{ nm}$ ^[165]. This represents a significant step towards controlled, high-resolution fiber placement compared to traditional electrospinning. Another technology based on the same principle is EHDJ. EHDJ manipulates fluid behavior using high electric fields, enabling microscale and even nanoscale high-resolution printing. When the applied voltage exceeds a threshold, a jet emerges from the tip, allowing precise deposition of droplets or continuous microjets onto the substrate.

An innovative manufacturing process for flexible transparent electrodes (FTEs) was introduced, achieving low-cost, high-efficiency, and environmentally friendly integrated fabrication. Initially, a layer of liquid PDMS is spin-coated onto the surface of a flexible substrate. Subsequently, an ultrathin metal mesh is directly printed onto the liquid film substrate using a liquid-substrate electric-field-driven microscale 3D printing process (Figure 6(c))^[166]. After low-temperature sintering, FTEs with excellent optoelectronic performance are obtained, exhibiting a sheet resistance of $6 \Omega \cdot \text{sq}^{-1}$ and a transmittance of 85.79%. This technology demonstrates exceptional mechanical stability and environmental adaptability under harsh working conditions, offering a novel manufacturing strategy for applications in flexible electronics, transparent heating, and sensors^[78,170,171].

To address the limitations of EHDJ in material compatibility, a 3D nanoprinting method employing charged

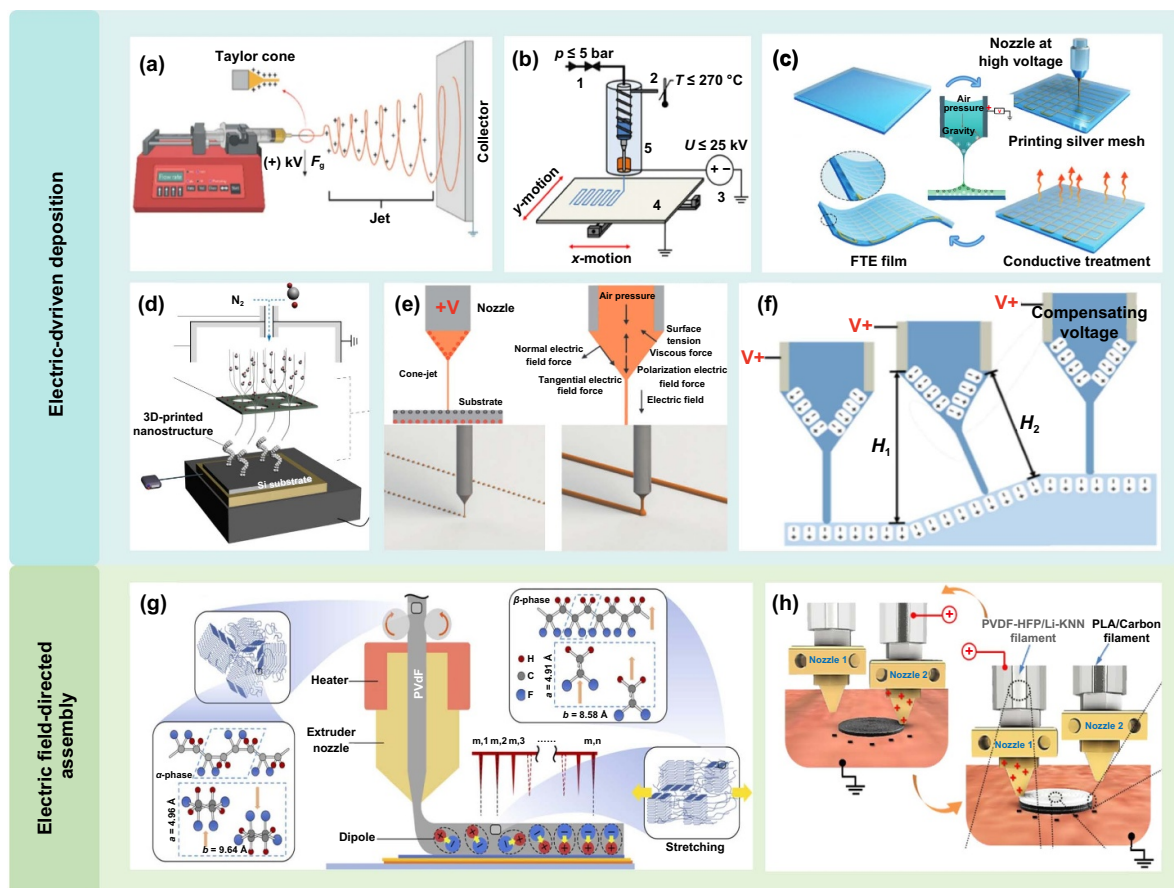


Figure 6. Electric field-assisted nozzle-based AM. (a) Example of electrospinning. Reproduced from^[164]. CC BY 4.0. (b) Melt electrowriting technology. Reproduced from^[165]. © IOP Publishing Ltd. CC BY 3.0. (c) Fabrication process of FTE. Reproduced from^[166]. CC BY 4.0. (d) 3D nanoprinting method with electrically assisted aerosol jet printing. Reproduced from^[167], with permission from Springer Nature. (e) EHDJ system with pulsed and continuous operation modes. Reproduced with permission from^[168]. Copyright 2020, Mary Ann Liebert, Inc., publishers. (f) Inclined plane EHDJ printing at varying tilt angles. Reprinted from^[68], Copyright (2024), with permission from Elsevier. (g) Schematic of the EPAM printing mechanism. Reprinted from^[69], Copyright (2022), with permission from Elsevier. (h) Low-voltage-assisted 3D printing technique for bulk ferroelectric metamaterials. Reprinted (adapted) with permission from^[169]. Copyright (2021) American Chemical Society.

aerosol jets was developed. This technique enables high-precision fabrication of metal nanostructures by utilizing an electric field to control nanoscale aerosol particles passing through a dielectric mask with micropores, achieving direct patterning of adjustable 3D geometries on a substrate. By eliminating reliance on polymer-based or solution-phase inks, this method enhances material purity and provides a new pathway for high-resolution electronics and sensor manufacturing. Furthermore, the established nanoscale jetting precision lays the groundwork for future advancements in advanced electric-field control strategies (Figure 6(d))^[167]. The aerosol-jet approach expands the material palette for EHDJ nanoprinting, offering a route to high-purity metallic structures with impressive resolution. Additionally, Zhang et al. introduced two operating modes—pulsed cone-jet mode and continuous cone-jet mode—tailored for printing low-viscosity and high-viscosity materials, respectively (Figure 6(e))^[168]. Experimental results showed that this method generates stable jet streams on various substrates. It successfully fabricates structures such as metallic mesh transparent electrodes, high-aspect-ratio walls, tissue engineering scaffolds,

and sensors^[160,172]. These advancements further expand the application scope of EHDJ, highlighting its suitability and advantages in microscale fabrication.

To explore the stability of EHDJ, the influence of nozzle electric field intensity on jet behavior and linewidth was investigated across substrates with varying inclination angles (10° – 25°). It was found that the ejected jet remains consistently perpendicular to the substrate surface, and slight voltage compensation ensures consistent linewidth in printed fibers, maintaining EHDJ stability (Figure 6(f))^[68]. Current EHDJ technology is capable of utilizing charge-induced self-alignment to match the printed linewidth with myocardial fiber dimensions, achieving fiber diameters of $20\ \mu\text{m}$ and inter-fiber spacings of $60\ \mu\text{m}$, which effectively promotes the maturation of engineered cardiac tissue^[173].

EPAM is typically integrated with direct writing or jet printing techniques. During the printing process, a poling field is applied to control material orientation and enhance both electrical and mechanical properties. Figure 6(g) clearly illustrates the core mechanism of EPAM: during deposition, the applied electric field aligns the dipoles within the material

along the field direction, imparting stable piezoelectric or ferroelectric properties to the final printed structure. This process ensures material functionality while enabling the direct formation of polarized regions during printing, eliminating the need for additional post-processing steps^[69]. The results indicate that the optimized EPAM process allows precise control over material polarization, thereby enhancing the electrical response of the final structure. This method provides an experimental foundation for EPAM and has been further refined in subsequent studies. Li et al. introduced a bulk ferroelectric metamaterial with enhanced piezoelectric and biomimetic mechanical properties using low-voltage-assisted 3D printing. The printing process involves creating a lamellar structure with alternating soft ferroelectric layers and hard electrode layers. During printing, an electric field is applied between the nozzle and the conductive layer, enabling in situ poling of the ferroelectric material (Figure 6(h)). This method facilitates the fabrication of a material with a significantly enhanced piezoelectric charge coefficient exceeding $150 \text{ pC}\cdot\text{N}^{-1}$ and a fracture toughness of approximately $5.5 \text{ MPa}\cdot\text{m}^{1/2}$, which is more than three times higher than that of conventional piezoceramics. These studies demonstrate the potential for creating high-performance piezoelectric materials with tunable anisotropic properties and bone-comparable mechanical characteristics, suitable for applications such as artificial bone implants and energy harvesters^[169,174].

Collectively, the various nozzle-based EFAM techniques discussed leverage the capabilities of electric fields to facilitate precise material manipulation and deposition. This includes established methods such as electrospinning, which has been utilized for fiber generation, alongside more recent direct-write approaches like MEW and EHDJ that permit the fabrication of sub-micron and nanoscale features. Furthermore, specialized strategies such as aerosol jetting offer enhanced material compatibility, and EPAM provides avenues for in-situ functionalization.

2.4.2. Vat photopolymerization-based EFAM. Unlike nozzle-based EFAM, the incorporation of electric fields in VPP-based AM requires careful consideration of the dielectric properties of the resin, the polarization behavior of fillers, and their interactions within the electric field. First, the dielectric constant and conductivity of the photocurable resin determine its response to the applied electric field and whether the field can effectively drive material deposition or self-assembly. Second, the alignment, dispersion, and orientation of fillers under the electric field directly influence the anisotropy, electrical performance, and mechanical strength of the printed structures. Thus, integrating electric fields with VPP-based AM not only involves light-induced polymerization but also requires coordinated control over filler manipulation to optimize the microstructure and macroscopic properties of the final material. EPD utilizes an electric field to direct charged particles suspended in a liquid photocurable resin toward selective deposition and solidification, enabling high-precision composite printing. In contrast, the electric field-directed assembly method manipulates the distribution

of filler particles through field-induced alignment, allowing composite materials to achieve controlled anisotropic structures during printing. These two approaches highlight the distinct functionalities of electric fields in VPP-based AM, offering new possibilities for fabricating high-performance electronic or stimuli-responsive materials.

In recent years, EPD has been integrated into AM to enable precise control over electric field distribution, facilitating the fabrication of complex 3D structures. Compared to EPAM, EPD offers advantages such as broad material compatibility, high deposition rates, and a relatively simple process, making it particularly suitable for the fabrication of highly filled nanocomposites. Researchers have continuously optimized EPD techniques to enhance their precision and applicability in AM.

Among them, Pan et al. proposed a Projection Electrophoretic Solidification (PES) method, advancing the application of EPD in polymer-particle composite fabrication. The PES approach combines electrostatic deposition with projection-based photopolymerization. A photoconductive film selectively collects charged particles in illuminated regions and transfers them into a photocurable resin layer, enabling precise particle distribution within the polymer matrix. The key innovation of this method lies in its ability to locally control multi-material composite dispersion and facilitate the fabrication of complex geometries by combining electrostatic deposition with photopolymerization (Figure 7(a))^[175]. The PES method enhanced EPD spatial resolution using light-patterned photoconductive surfaces for composite fabrication.

Seeking to enhance the flexibility of such light-directed approaches, Pascall et al. further developed light-directed EPD by utilizing a photoconductive electrode as a dynamically adjustable component, overcoming the fixed constraints of photomask-based techniques and allowing flexible control over electric field regions (Figure 7(b)). This approach significantly improved the adaptability of the deposition process, particularly in multi-material deposition and programmable patterning. Moreover, their study combined experimental and simulation-based analyses to investigate the influence of electric field gradients on particle orientation, providing crucial theoretical insights for subsequent research^[176]. To further optimize the integration of projection-based photopolymerization and electric fields, Mora et al. introduced a projection-assisted EPD method, where a photomask was used to modulate electric field distribution, enabling precise nanoparticle deposition (Figure 7(c)). The key innovation of this approach lies in the synergistic effect of light and electric fields, allowing particles to be precisely positioned at the micro-scale, thus overcoming the traditional limitation of EPD being constrained by electrode geometry^[177]. This study not only improved the resolution of EPD in 3D structure fabrication but also laid the foundation for future exploration of more sophisticated electric field control strategies. Employing dynamic electrodes or light-modulated fields offered more versatile and higher-resolution EPD. Implementing such dynamic control for complex 3D structures, however, requires sophisticated system integration and understanding of complex particle-field interactions.

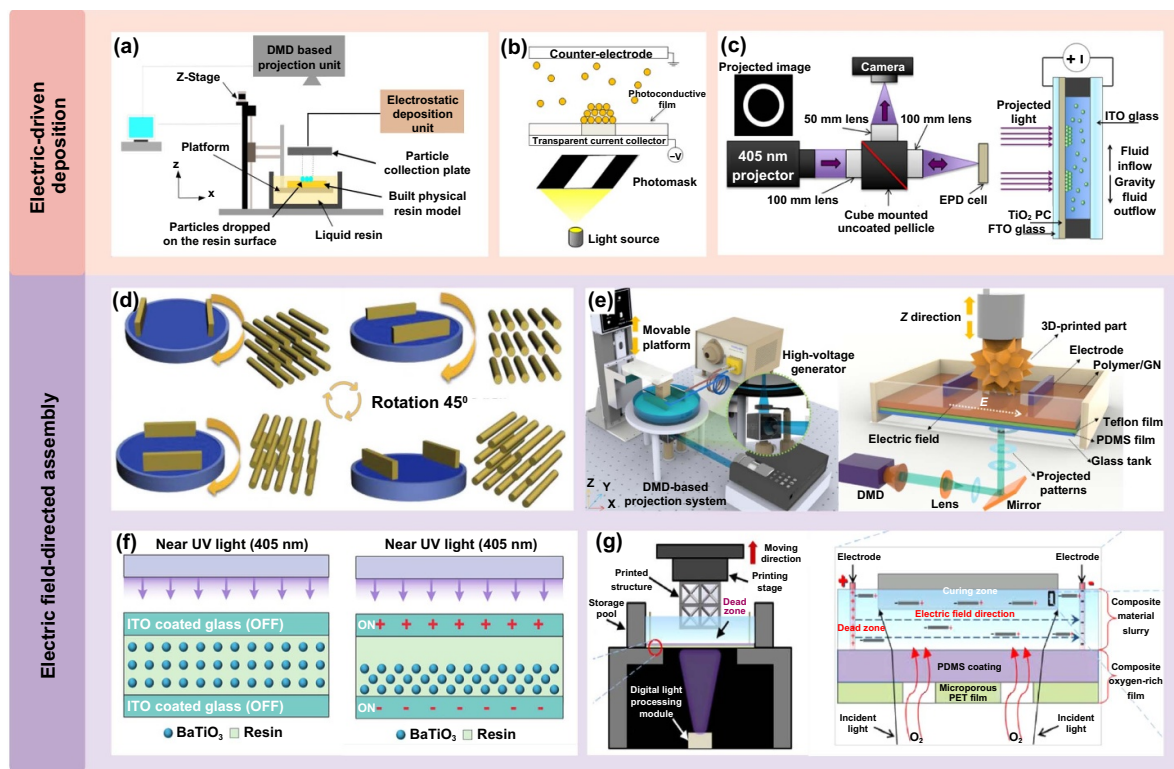


Figure 7. Electric field-assisted VPP-based AM. (a) Projection electrophoretic sedimentation method. Used with permission of EMERALD GROUPELLUBLISHING LIMITED, from^[175]; permission conveyed through Copyright Clearance Center, Inc. (b) Light-guided EPD technique. Reproduced with permission from^[176]. © 2015 Trans Tech Publications Ltd. All Rights Reserved. (c) EPD method employing photomasks to modulate the electric field distribution. Reprinted from^[177], Copyright (2018), with permission from Elsevier. (d) Schematic illustrating the orientation alteration of MWCNT-S induced by electrode rotation. ^[162] John Wiley & Sons. © 2017 WILEY-VCH Verlag GmbH & Co. KGaA, Weinheim. (e) Bottom-up electric field-assisted projection SLA system. From^[81]. Reprinted with permission from AAAS. (f) Process steps for fabricating hierarchical composites using electric field-assisted SLA methods. Reprinted from^[178], Copyright (2023), with permission from Elsevier. (g) Electric field-assisted continuous VPP 3D printing technology. Reprinted from^[179], Copyright (2023), with permission from Elsevier.

The introduction of an electric field can not only drive the migration of charged particles but also manipulate the alignment of fillers to fabricate anisotropic composite materials. This process relies on the reorientation of internal dipole moments within the material under an applied electric field, which subsequently influences the distribution and alignment of fillers such as magnetic nanoparticles, dielectric particles, or conductive fillers before resin solidification. By precisely controlling the intensity, frequency, and direction of the applied field, fillers can be aligned in predefined patterns, endowing the final material with anisotropic electrical, magnetic, or mechanical properties. This strategy is particularly valuable for fabricating stimuli-responsive materials, anisotropic conductive materials, and functionally graded composites. In recent years, significant progress has been made in electric field-assisted VPP-based AM technology. Yang et al. have continuously expanded the application boundaries of this technology through a series of studies. In their early work, they utilized an electric field-assisted nanocomposite 3D printing technique. By means of a rotating electric field, they achieved the dynamic alignment of surface-modified multi-walled carbon nanotubes (MWCNT-S) in a polymer matrix^[162]. As shown in Figure 7(d), after applying a direct current voltage,

MWCNT-S are affected by the electric field and change their alignment directions as the electrodes rotate, ultimately constructing a composite material with a biomimetic Bouligand structure. Their research revealed that precisely controlling the alignment direction of MWCNT-S in each layer and the rotation angle between adjacent layers can effectively regulate the mechanical properties of the material.

Subsequently, Yang et al. delved deeper into the research. They employed electric field-assisted 3D printing technology to fabricate a nacre-inspired structure with self-sensing capabilities^[81]. Figure 7(e) demonstrates the experimental setup and the bottom-up projection-based SLA process. During this process, a $433 \text{ V}\cdot\text{cm}^{-1}$ electric field aligns graphene nanoplatelets in the photocurable resin, forming a 'brick-mortar' structure similar to nacre. This structure not only endows the material with lightweight, high-strength, and high-toughness characteristics but also imparts excellent electrical conductivity in specific directions, enabling self-sensing functionality. Zhong et al. took a different approach and applied the electric field-assisted VPP-based AM technology to the microelectronics packaging field. The left part of Figure 7(f) shows the conventional preparation process of a uniformly dispersed BaTiO₃-resin composite, which is a

relatively basic preparation process. Specifically, a resin containing BaTiO₃ particles is cured by near-ultraviolet light for 20 minutes to form the composite. The right part of Figure 7(f), however, displays the key step of fabricating a graded composite using an electric field-assisted SLA method. Under a 100 V·mm⁻¹ direct current electric field, BaTiO₃ particles migrate and aggregate in the resin matrix due to the potential difference between the electrodes. After another 20 minutes of near-ultraviolet light curing, a graded BaTiO₃-resin composite with unique properties is obtained, providing new ideas for the development of microelectronics packaging materials^[178].

In addition, Zhang et al. actively explored innovative applications of the electric field-assisted VPP-based AM technology. They proposed an electric field-assisted continuous VPP 3D printing technique, aiming to fabricate high-performance ordered graphene/polymer composites^[179]. The left part of Figure 7(g) shows the 3D printing system platform, which integrates multiple components such as a DLP module and a storage tank, forming a complex and precise printing system. The right part of Figure 7(g) shows the alignment change of graphene under the action of an electric field during the printing process. During printing, the composite oxygen-rich film creates a 'dead zone' and an uncured thin liquid layer in the photocurable resin. When an electric field is applied, the randomly distributed graphene nanoplatelets polarize and align along the direction of the electric field. By optimizing parameters such as the graphene content, printing speed, and light intensity, Zhang et al. successfully achieved the continuous fabrication of composite materials. Experimental data shows that compared with pure polymers, the ordered 2 wt% graphene/polymer composite exhibits a 101% increase in tensile strength and a 15-fold increase in electrical conductivity. This provides an efficient new method for the preparation of such composite materials and further promotes the development of electric field-assisted VPP-based AM technology.

EFAM leverages electrostatic forces and electrophoretic effects to achieve precise material manipulation, excelling in micro/nano-scale fabrication, functional material integration, and multi-material composites. Its core innovation lies in two mechanisms: electric field-driven deposition and electric field-induced self-assembly. EHDJ forms stable jets via high-voltage electric fields to produce nanoscale droplets or fibers, while EPD combined with photopolymerization guides charged particles for high-resolution 3D composite structures, overcoming traditional electrode geometry constraints. Electric field-induced self-assembly aligns dipoles to impart piezoelectric or ferroelectric properties, significantly enhancing mechanical and functional performance. Unlike magnetic fields, electric fields rely on charge/ion responses in the medium, extending applicability to non-magnetic materials. By tuning electric field strength, direction, and frequency, EFAM synchronizes microstructural alignment and macroscopic functionality. Technologically, nozzle-based systems control droplet morphology and fiber orientation, while vat-based systems integrate electric fields with light to dynamically align fillers, such as electrically tuned porous structures. EFAM's breakthrough lies in multifunctional

integration, offering high-precision, cost-effective pathways for flexible electronics, smart sensors, and biomedical devices. Future advancements must address challenges in electric field uniformity, multi-field synchronization, and dispersion stability of high-concentration fillers. Overcoming these issues is key to realizing the full potential of high-performance composites and bioinspired functional architectures.

2.5. Comparison and summary of FAM

After introducing the fundamental principles and manufacturing processes of MFAM, AFAM, and EFAM in Sections 2.2–2.4, this section provides a summary and comparison of these three FAM approaches. Section 2.5.1 highlights the capabilities and performance of MFAM, AFAM, and EFAM, focusing on their typical resolutions, main technical characteristics, representative applications, and functional enhancements, as summarized in Table 2. Section 2.5.2 discusses the limitations and challenges of each method, emphasizing material compatibility, process limitations, and system integration challenges, which are comparatively outlined in Table 3.

2.5.1. Capabilities and performance of FAM.

MFAM, AFAM, and EFAM represent three leading strategies in next-generation functional device fabrication, each distinguished by its unique achievable resolution, technical characteristics, and application areas (Table 2). MFAM leverages magnetic fields to enable non-contact manipulation and programmable alignment of magnetic particles within composites, supporting the fabrication of structures with user-defined magnetic anisotropy and multi-material gradient magnetization. The typical resolution for MFAM is above 100 μm^[100], which is sufficient for many soft robotics and functional composite applications, though it is less suited for ultra-fine micro/nano structuring. AFAM utilizes acoustic waves to achieve non-contact, real-time alignment of cells, fibers, and particles, enabling the precise self-assembly of multi-material microstructures and the fabrication of biomimetic, anisotropic tissue-like constructs. AFAM can reach resolutions as fine as 5.71 μm^[93], making it highly suitable for tissue engineering scaffolds, microfluidic devices, and other applications requiring fine spatial control. EFAM employs electric fields to achieve high-precision, non-contact alignment of conductive fillers and direct printing of conductive polymers or biomimetic structures. With a typical resolution down to 100 nm^[180], EFAM stands out for its ability to fabricate micro/nanoscale electronic components, piezoelectric and ferroelectric devices, and flexible electronics with enhanced functional properties.

In terms of application focus and demonstrated performance, each FAM approach offers unique advantages. MFAM is particularly effective for soft robotics, untethered microrobots, programmable actuators, and magnetic sensors, where programmable magnetic anisotropy and remote actuation are essential. For example, MFAM has enabled the fabrication of flexible multi-legged robots with a 6.8-fold increase

Table 2. Summary of key functionalities, representative applications, and performance enhancements of FAM.

Technology	Resolution	Key functionalities	Representative applications	Performance enhancement
MFAM	$>100 \mu\text{m}^{[100]}$	<ul style="list-style-type: none"> • Non-contact manipulation of magnetic particles within composites • Programmable printing of structures with magnetic anisotropy • Manufacturing magnetically responsive composites with user-defined magnetization curves • Fabrication of multi-material gradient magnetized structures 	<ul style="list-style-type: none"> • Soft robotics • Untethered microrobots • Programmable actuators • Magnetic sensors • Functionally graded materials • Printed magnets 	<ul style="list-style-type: none"> • MFAM achieves flexible multi-legged robots with a 6.8-fold increase in stride length (up to 3.8 mm) and superior rugged terrain navigation compared to conventional magnetic actuators^[67] • MFAM enables the fabrication of P-TPMS lattice sensors with tunable sensitivity ranging from $0.75 \mu\text{V}\cdot\text{mm}^{-1}\cdot\text{min}$ to $1.79 \mu\text{V}\cdot\text{mm}^{-1}\cdot\text{min}^{[101]}$
AFAM	$>5.71 \mu\text{m}^{[93]}$	<ul style="list-style-type: none"> • Non-contact manipulation and alignment of cells, fibers, and particles • Fabrication of biomimetic, anisotropic tissue-like structures • Precise self-assembly of multi-material microstructures • Direct in vivo printing of tissues and organs 	<ul style="list-style-type: none"> • Biofabrication • Tissue engineering scaffolds • Anisotropic composites • Embedded multi-material structures • Microfluidic devices 	<ul style="list-style-type: none"> • AFAM enables silver ink printing with a line width of $5.71 \mu\text{m}$ and overspray of $0.08 \mu\text{m}$, reducing line width by 60% compared to without acoustic field^[93] • Ultrasonic vibration-assisted printing reduces viscosity by up to 30%, achieving 98% fidelity and sub-micron resolution for high-viscosity materials^[90]
EFAM	$>100 \text{nm}^{[180]}$	<ul style="list-style-type: none"> • Non-contact, high-precision alignment of conductive fillers • Polarization-enabled fabrication of piezoelectric composites • Direct printing of conductive polymers or biomimetic structures • Reorientation of dipoles for enhanced functional properties 	<ul style="list-style-type: none"> • Piezoelectric devices • Ferroelectric devices • Flexible electronics • Conductive polymer devices • Electrode manufacturing 	<ul style="list-style-type: none"> • EFAM enables the fabrication of sub-micron fiber scaffolds^[165] • EFAM produces piezoelectric devices with an average piezoelectric response of $47.76 \text{pC}\cdot\text{N}^{-1}$ in force-sensitive matrices^[69]

Table 3. Comparison of FAM in terms of material, limitations and integration challenges.

Technology	Material compatibility	Particle distribution	Process challenges	System integration challenges
MFAM	<ul style="list-style-type: none"> Matrix materials: Silicone rubber, UV resin, etc. Reinforcement phases: Fe₃O₄ magnetic particles, ferrite permanent magnetic particles, etc. Narrow material window (Magnetic property dependence) 	<ul style="list-style-type: none"> Arranged along 3D magnetic field lines or gradients Sensitive to particle size, shape, and uniformity of the field 	<ul style="list-style-type: none"> Viscosity increase Nozzle clogging Particle aggregation Few filler materials Limited magnetic field range 	<ul style="list-style-type: none"> Electromagnetic and physical interference Electromagnet cooling system integration Stable, continuous, and possibly uniform magnetic field generation
AFAM	<ul style="list-style-type: none"> Matrix materials: Epoxy resin, hydrogel, etc. Reinforcement phases: Silver nanoparticles, cell microspheres, etc. Widest material window (Low material property dependence) 	<ul style="list-style-type: none"> Particles concentrate at the nodes of the acoustic field Planar distribution; difficult to achieve vertical distribution 	<ul style="list-style-type: none"> Acoustic attenuation Flow instability Acoustic thermal Limited 3D acoustic field 	<ul style="list-style-type: none"> Transducer design and integration in platforms and resin tanks Transducer cooling in high frequency acoustic fields Acoustic reflection and resonance interference Harmonization of the time of action of different acoustic effects
EFAM	<ul style="list-style-type: none"> Matrix materials: PDMS, Polylactic acid, etc. Reinforcement phases: Conductive nanoparticles, carbon nanotubes, etc. Moderate material window (Electrical conductivity dependence) 	<ul style="list-style-type: none"> Arranged along electric field lines or gradients. Polymer/particle dipole polarization and alignment Tip aggregation 	<ul style="list-style-type: none"> Electrothermal effects Electrical breakdown Material deposition Low printing efficiency 	<ul style="list-style-type: none"> High voltage power source stabilization and control Electromagnetic and physical interference Joule heat and electrochemical reaction control and avoidance Electric field crosstalk in multi-nozzle printing

in stride length (up to 3.8 mm) and superior rugged terrain navigation compared to conventional magnetic actuators, as well as primitive TPMS (P-TPMS) lattice sensors with tunable sensitivity ranging from $0.75 \mu\text{V}\cdot\text{mm}^{-1}\cdot\text{min}$ to $1.79 \mu\text{V}\cdot\text{mm}^{-1}\cdot\text{min}$ ^[67,101]. AFAM excels in biofabrication, tissue engineering scaffolds, and the creation of anisotropic composites and embedded multi-material structures. Notably, AFAM has achieved silver ink printing with a line width of $5.71 \mu\text{m}$ and overspray of $0.08 \mu\text{m}$, representing a 60% reduction in line width compared to processes without acoustic field assistance^[93]. Additionally, ultrasonic vibration-assisted printing in AFAM can reduce material viscosity by up to 30%, achieving 98% fidelity and submicron resolution for high-viscosity materials^[90]. EFAM is the method of choice for piezoelectric and ferroelectric devices, flexible electronics, and electrode manufacturing, where ultra-high resolution and precise alignment are required. EFAM has demonstrated the fabrication of sub-micron fiber scaffolds^[165], and piezoelectric devices with an average response of $47.76 \text{pC}\cdot\text{N}^{-1}$ in force-sensitive matrices^[69].

Overall, these field-assisted AM techniques significantly expand the functional and structural capabilities of AM, enabling the creation of devices and materials with tailored properties and enhanced performance. The specific application domains and quantitative improvements highlighted here are further explored in detail in Section 3.

2.5.2. Limitations and challenges of FAM. Despite the remarkable improvements that FAM brings, every approach faces specific limitations and practical challenges. Material compatibility has different limitations in the three fields. MFAM is highly dependent on the magnetic properties of the matrix and reinforcement phases, typically requiring the use of silicone rubber, UV resin, and magnetic fillers such as Fe_3O_4 or ferrite particles^[59,66]. This results in a relatively narrow material window, restricting the diversity of functional materials that can be processed. In contrast, AFAM offers the broadest material compatibility, as it can process a wide range of matrix materials, including epoxy resins and hydrogels, and reinforcement phases such as silver nanoparticles and cell microspheres^[140,181], due to its low dependence on specific material properties. EFAM occupies a middle ground, with moderate material compatibility that is largely determined by the electrical conductivity of the matrix and fillers, such as PDMS, polylactic acid, and conductive nanoparticles^[78]. This electrical property dependence limits the range of usable materials, especially for applications requiring non-conductive or biocompatible matrices.

The ability to control particle distribution and overcome process-related challenges is another critical bottleneck for FAM technologies. In MFAM, the alignment of particles along 3D magnetic field lines is highly sensitive to particle size, shape, and the uniformity of the applied field. This can lead to issues such as particle aggregation, nozzle clogging, and increased viscosity, which in turn limit the range of filler materials and the overall process stability. AFAM, while

excelling in planar particle alignment at the nodes of the acoustic field, faces difficulties in achieving vertical distribution and is susceptible to acoustic attenuation, flow instability, and thermal effects. These factors can restrict the fabrication of truly 3D structures and affect the fidelity of complex architectures. EFAM relies on the arrangement of particles along electric field lines and the polarization of polymer or particle dipoles, but is challenged by tip aggregation, electrothermal effects, and the risk of electrical breakdown. Long print times resulting in material deposition and low print efficiencies further limit the scalability and reliability of the EFAM process.

System integration and actuation control present additional hurdles for the practical deployment of FAM. MFAM systems must address electromagnetic and physical interference, the need for stable and uniform magnetic field generation, and the integration of cooling systems for high-power electromagnets. These requirements increase system complexity and may limit scalability. AFAM requires precise transducer design and integration within platforms and resin tanks, as well as effective cooling in high-frequency acoustic fields. Acoustic reflection, resonance interference, and the harmonization of different acoustic effects further complicate system control. For EFAM, high-voltage power stabilization, electromagnetic interference, and the management of Joule heating and electrochemical reactions are major concerns. Additionally, electric field crosstalk in multi-nozzle printing setups can compromise process accuracy and device performance. Collectively, these system-level challenges highlight the need for further innovation in hardware design, real-time control strategies, and multi-physics integration to fully realize the potential of FAM in advanced manufacturing.

3. Micro/nano device applications of FAM

FAM has emerged as a transformative technology for the fabrication of MNDs, offering unprecedented precision, structural control, and functional integration capabilities. By leveraging external fields such as magnetic, acoustic, and electric fields, FAM enables the manipulation of materials at the micro- and nanoscale with enhanced accuracy and efficiency^[15,33,34]. This capability addresses key challenges in traditional manufacturing techniques, including limited geometric complexity, poor material uniformity, and insufficient functional performance.

MNDs play a pivotal role in advancing cutting-edge technologies across various domains, including biomedical engineering^[182,183], flexible electronics^[26], and microrobotics^[184–186]. These devices often require intricate architectures, tailored material properties, and multifunctional designs to meet the demands of specific applications. For instance, in biomedical implants, high biocompatibility and precise drug delivery mechanisms are crucial, while in micro/nano electronic sensors, reliable conductivity and sensitivity are essential. FAM's ability to achieve fine-tuned material alignment, optimize structural configurations, and integrate multiple functionalities makes it particularly well-suited for these demanding applications.

This section systematically explores the diverse applications of FAM in micro/nano device fabrication, focusing on three key areas: (i) micro/nanorobots, which hold great promise for smart healthcare and environmental monitoring; (ii) biomedical devices, where FAM facilitates the production of high-performance implants, tissue scaffolds, and drug delivery systems; and (iii) micro/nano electronic sensors, which benefit from FAM's high-precision patterning and assembly capabilities. Through detailed case studies, we highlight how FAM enhances fabrication precision, improves material properties, and enables innovative functionalities in these fields.

3.1. Micro/nanorobots

Micro/nanorobots have vast potential in fields such as smart healthcare, environmental monitoring, and precision manufacturing^[187,188]. Their core functional requirements primarily stem from the diversity of their movement modes. Micro/nanorobots can move freely in complex environments through various movement modes, such as crawling, rotation, rolling, sliding, and walking^[189–191]. These movement modes allow them to not only adapt to a wide range of complex tasks, but also navigate challenges such as obstacles, fluid flows, or sticky surfaces. With advancements in technology, many micro/nanorobots are now capable of performing multimodal movements, combining various modes to execute tasks efficiently. Multimodal movement enables micro/nanorobots to choose the most appropriate motion strategy in different working environments. For example, in minimally invasive surgery, micro/nanorobots may need to roll and crawl within blood vessels for precise operations, while in environmental monitoring, they may use crawling and sliding to navigate through complex terrains. In addition to mobility, the functional requirements of micro/nanorobots also include multifunctionality and adaptability. To accomplish diverse tasks, micro/nanorobots must be capable of functions such as targeted drug delivery, minimally invasive surgery, and environmental pollution monitoring, and must adjust their behavior in response to external signals or environmental changes. By integrating sensors, actuation systems, and control units, micro/nanorobots can perceive and respond to environmental changes in real time, ensuring the smooth execution of tasks. Lastly, micro/nanorobot design must consider material biocompatibility, flexibility, and intelligent responsiveness. These factors ensure stable operation in practical applications and help prevent adverse reactions during interactions with biological systems or environments^[192,193].

Despite significant advancements in traditional AM technologies, such as SLA and FDM, these techniques still face several limitations when it comes to the fabrication of micro/nanorobots. First, traditional AM methods often fail to provide the necessary precision at micro and nano scales, which is crucial for high-precision positioning and control in microrobotics. Micro/nanorobots typically require precise fabrication at the micron and even nanometer levels, but the resolution of conventional AM methods is often insufficient to meet this need^[117,194]. Furthermore, the material compatibility of traditional AM techniques is limited. Many conventional AM

processes can only work with a restricted range of materials, which restricts the development of multifunctional micro/nanorobots. Micro/nanorobots often require the integration of different functional materials, such as magnetic, conductive, and biocompatible materials, which go beyond the capability of traditional AM methods. Additionally, traditional AM technologies are typically unable to effectively perform multi-material printing, particularly at the micro/nano scale, where the precise combination of materials is essential for meeting the multifunctionality requirements of micro/nanorobots. Lastly, traditional AM techniques often exhibit limited production speed and control over the manufacturing process, particularly in complex tasks that require dynamic adjustments, making it difficult to achieve efficient control and precise operation of micro/nanorobots.

In micro/nanorobot fabrication, FAM empowers traditional AM techniques by introducing external fields, such as magnetic and acoustic fields, to achieve precision and multifunctionality that traditional methods cannot reach. Magnetic and acoustic fields enable precise control over materials, particularly at the micro scale, significantly expanding the capabilities of micro/nanorobot manufacturing. The introduction of magnetic fields allows for the accurate manipulation of materials containing magnetic fillers or particles, enabling micro/nanorobots to adjust their position and orientation in response to external magnetic fields. This ability is crucial for tasks such as microrobot navigation, precise localization, and task execution. For instance, by applying an external magnetic field, micro/nanorobots can autonomously navigate through complex environments, including blood vessels and tissues, enabling precise drug delivery and minimally invasive surgery. This unique empowering mechanism gives FAM a significant advantage over traditional AM techniques when it comes to fabricating complex micro/nanorobots.

FAM has achieved significant results and breakthroughs in the fabrication of micro/nanorobots. In crawling locomotion, a magLCE strip robot fabricated via magnetic-field-assisted 3D printing demonstrates temperature-responsive behavior. Its motion mechanism arises from the synergy of programmable magnetization and LCE nematic order. At room temperature, magnetic actuation drives crawling via leg deformation; at 100 °C, the material undergoes phase transformation to form a tubular shape and rotates via twisting under magnetic fields. At 150 °C, thermally induced autonomous propulsion enables self-driven motion without external fields (Figure 8(a))^[108]. Magnetic soft robots with distributed optical fiber sensors achieve dynamic deformation and navigation by real-time strain monitoring and closed-loop magnetic control, enabling obstacle avoidance in enclosed pipelines (Figure 8(b))^[195]. For terrain adaptation, groove-structured magnetic flexible multi-legged robots exhibit enhanced deformation under magnetic fields: horizontal leg amplitude increases from 0.49 mm to 4.05 mm (8.3×), vertical amplitude from 1.56 mm to 8.87 mm (5.7×), and stride length from 0.568 mm to 3.857 mm (6.8×), surpassing conventional magnetic actuators in rugged terrain navigation (Figure 8(c))^[67]. Magnetic encoding multi-layer robots integrate soft magnetic materials (SMM) and hard magnetic materials (HMM), enabling stable walking through

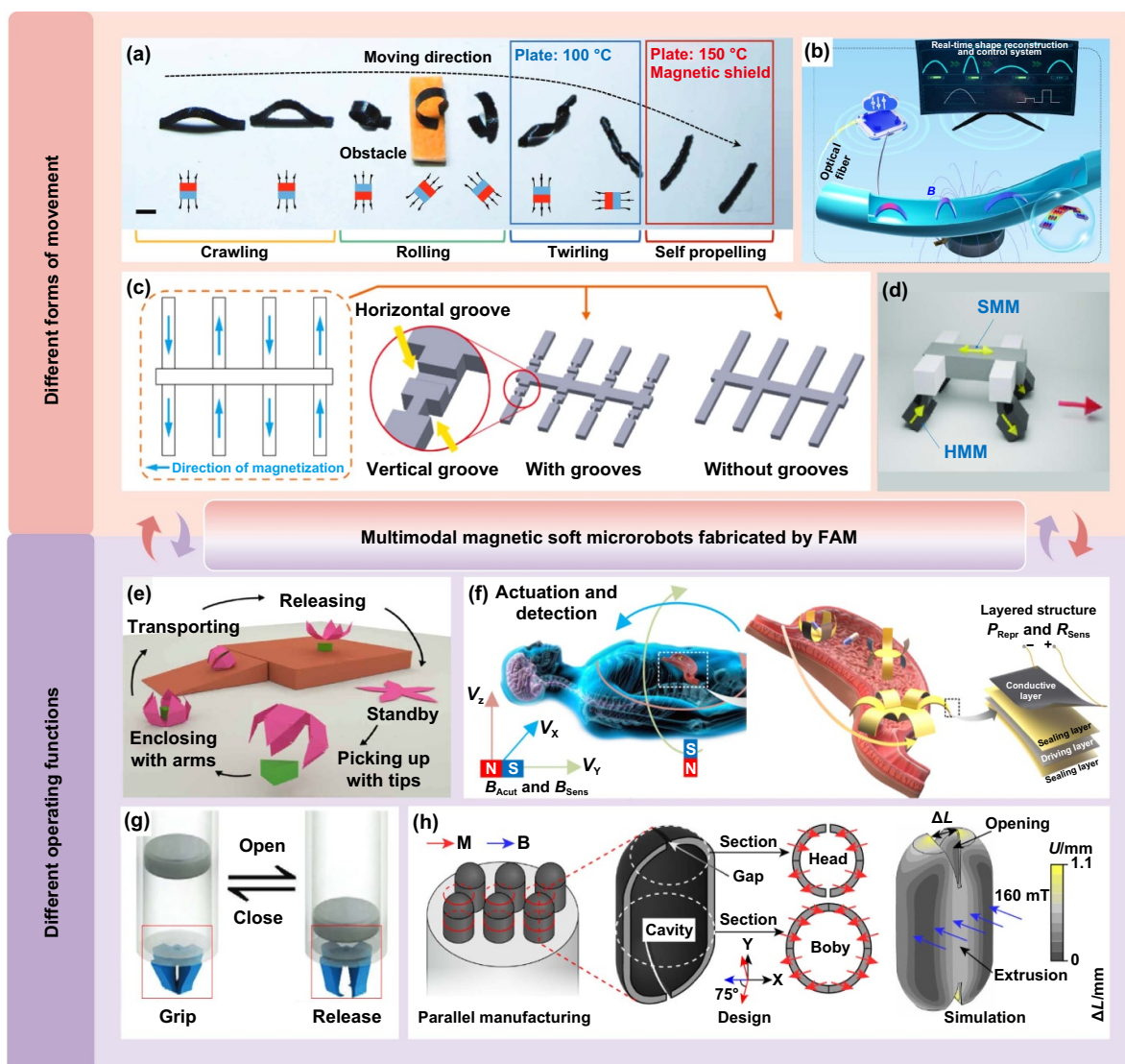


Figure 8. FAM for micro/nanorobots applications. (a) Temperature-responsive behavior of magLCE strip-shaped robots. [108] John Wiley & Sons. © 2023 Wiley-VCH GmbH. (b) Magnetic soft robots with distributed fiber-optic sensors. Reprinted (adapted) with permission from [195]. Copyright (2024) American Chemical Society. (c) Magnetic flexible multi-legged robots featuring grooved structures. Reprinted from [67], Copyright (2024), with permission from Elsevier. (d) Magnetically encoded multi-layered walking robots. Reproduced from [196]. CC BY 4.0. (e) 6-DOF magnetic microgrippers with transport and grasping capabilities. From [66]. Reprinted with permission from AAAS. (f) Multi-layered magnetic robots with drug-delivery functionalities. Reproduced from [197]. CC BY 4.0. (g) Magnetic microgrippers. [122] John Wiley & Sons. © 2022 Wiley-VCH GmbH. (h) Bioinspired capsule robots with radially magnetized navigation systems. Reproduced from [100]. CC BY 4.0.

coordinated leg bending. SMM provides orientation anchoring under oscillating fields, while HMM drives reciprocating motion, enhancing adaptability in complex environments (Figure 8(d)) [196].

FAM enables multifunctional capabilities such as grasping, transportation, ingestion, and expulsion through multi-material integration. A 6-DOF magnetic microgripper fabricated via DLP SLA and programmable magnetization achieves precise cargo handling: magnetic actuation folds the arms to grasp objects and releases them via field direction reversal (Figure 8(e)) [66]. For drug delivery, multi-layer magnetic robots with heating-sensing layers enable in-situ magnetization reprogramming via localized heating, coupled with

resistive position sensing (± 3 mm) and orientation sensing ($\pm 2.5^\circ$) under low magnetic fields (5 mT), successfully performing gastric drug delivery in simulated environments (Figure 8(f)) [197]. Magnetic particle distribution optimization via CVP achieves high uniformity and magnetic responsiveness, enabling precise gripper actuation (Figure 8(g)) [122]. Biomimetic capsule robots fabricated via uniform magnetic field-assisted SLA feature radial magnetization for navigation and a 300 μm slit for programmable drug release, preventing leakage during transport (Figure 8(h)) [100]. These functions synergize with motion modes: grasping relies on multi-axis actuation, while drug delivery integrates autonomous propulsion.

FAM overcomes traditional AM limitations by enabling multi-field synergy and material innovation, expanding micro/nanorobot capabilities in motion diversity and terrain adaptation through groove structures and magnetic encoding. Functionally, FAM integrates sensing, actuation, and multi-material systems for precise tasks such as drug delivery, obstacle-avoidance navigation, and high-precision cargo handling. Despite progress, improvements are needed in magnetic field continuity, multi-field control precision, and biocompatible material development. Future advancements in multi-field integration and cross-disciplinary innovation will further enhance micro/nanorobot precision, adaptability, and task complexity, driving breakthroughs in precision medicine and advanced manufacturing.

3.2. Biomedical devices

The design and fabrication of biomedical devices represent a critical intersection between engineering innovation and clinical needs, requiring precise alignment with the physiological characteristics of human tissues and specific repair objectives^[3,13]. Central to this effort is the seamless integration of biomimetic structures, dynamic functionalities, and gradient material properties. For instance, replicating the aligned architecture of myocardial fibers is essential for reconstructing electrical signal transmission, while balancing mechanical support with adaptive porosity is crucial for bone tissue regeneration^[133,169]. However, traditional manufacturing techniques often fall short of addressing these demands due to limitations such as insufficient resolution, material homogeneity issues, and static fabrication mechanisms^[198].

FAM enables unprecedented control over material alignment, structural complexity, and functional optimization at micro/nanoscales. This capability not only enhances the precision of biomimetic designs but also facilitates the integration of dynamic functionalities, such as stimuli-responsive behavior and gradient mechanical properties. Furthermore, FAM's compatibility with biocompatible materials and its ability to achieve high-resolution patterning make it particularly well-suited for biomedical applications.

This section explores the diverse applications of FAM in biomedical device fabrication, focusing on two primary domains: *in vitro* tissue model fabrication and *in vivo* bioprinting for functional repair. In the *in vitro* domain, FAM is utilized to construct biomimetic tissue models and tissue engineering scaffolds that replicate the native extracellular matrix, promoting cell growth, differentiation, and tissue regeneration. These scaffolds exhibit gradient porosity and mechanical compatibility, enabling precise control over structural and functional properties essential for laboratory studies and pre-clinical testing. In the *in vivo* domain, FAM facilitates direct bioprinting of tissues and organs at the site of injury, offering tailored solutions for functional tissue repair. Through detailed case studies, we demonstrate the advantages of FAM-manufactured biomedical devices and their functional integration capabilities, enabling enhanced performance in regenerative medicine applications.

FAM significantly enhances the precision and functionality of *in vitro* tissue models and tissue engineering scaffolds. In the fabrication of *in vitro* tissue models, dynamic interface printing has been employed to produce kidney-shaped hydrogel micro-nano devices with high cell viability (93%) without relying on complex feedback systems or specialized chemicals (Figure 9(a))^[71]. Additionally, ultrasound standing bulk acoustic waves enable precise directional alignment of cells, as demonstrated in a three-layer GelMA meniscus model that replicates tendon and cardiac tissue microstructures through controlled 0°–45°–90° cell orientations (Figure 9(b))^[133]. Acoustic radiation forces are utilized to pattern cell-extracellular matrix arrangements with high fidelity, offering robust platforms for drug screening and disease modeling. High-amplitude ultrasonic vibrations address high-viscosity material printing challenges, achieving sub-micron-resolution polymer clay crown models (Figure 9(c))^[90]. Ultrasonic vibration reduces material viscosity by 30%, enabling edge-intact prints with 98% fidelity. Additionally, ultrasound-driven bioprinting mimics meniscal circumferential cell alignment (Figure 9(d))^[132]. For tissue engineering scaffolds, MEW has been applied to fabricate sub-micron fiber scaffolds (Figure 9(e))^[165]. These scaffolds are coated with a reactive macromer, NCO-sP(EO-stat-PO), to ensure stable attachment during *in vitro* culture, even under frequent medium changes. Furthermore, electric field-driven microscale 3D printing achieves an accuracy of less than 100 μm , allowing the fabrication of tubular mesh structures with a diameter of 6 mm and a line width of 80 μm (Figure 9(f))^[199]. Voltage-controlled electric fields generate preset eccentricity in molten polymers, ensuring conformal printing on curved substrates. These structures exhibit shape memory characteristics and anisotropic modulus gradients with a 3:1 ratio, mimicking native myocardial mechanics.

FAM also enables minimally invasive and precise *in vivo* bioprinting and tissue repair. In *in vivo* bioprinting, magnetic soft catheter robots achieve high-precision implantation through superimposed magnetic fields, with access channels smaller than 5 mm (Figure 9(g))^[73]. NdFeB-PDMS composites maintain 98.6% cell viability, successfully modeling left atrial appendage closure and bone defect repair. The system adjusts catheter shape in real-time via external magnetic fields, achieving path accuracy within ± 50 microns. Direct acoustic printing leverages ultrasound-induced cavitation effects to enable non-invasive printing of deep-tissue structures without toxic additives. Focused ultrasound penetrated through 15 mm of tissue and 18 mm of PDMS to print a maple leaf pattern onto porcine skin (Figure 9(h))^[148]. Deep-penetration acoustic volumetric printing enables through-tissue drug delivery and bone repair by co-depositing paclitaxel-loaded microspheres and bioinks, creating hepatic tumor models with sustained release over four weeks and 40% improved suppression. Magnetic *in situ* printing boosts left ventricular ejection fraction by 23% in rat myocardial repair models, leveraging thermo responsive hydrogels that self-adapt to cardiac defects at 37 °C. Acoustically assembled liver lobule models achieve 89% drug metabolism prediction accuracy through

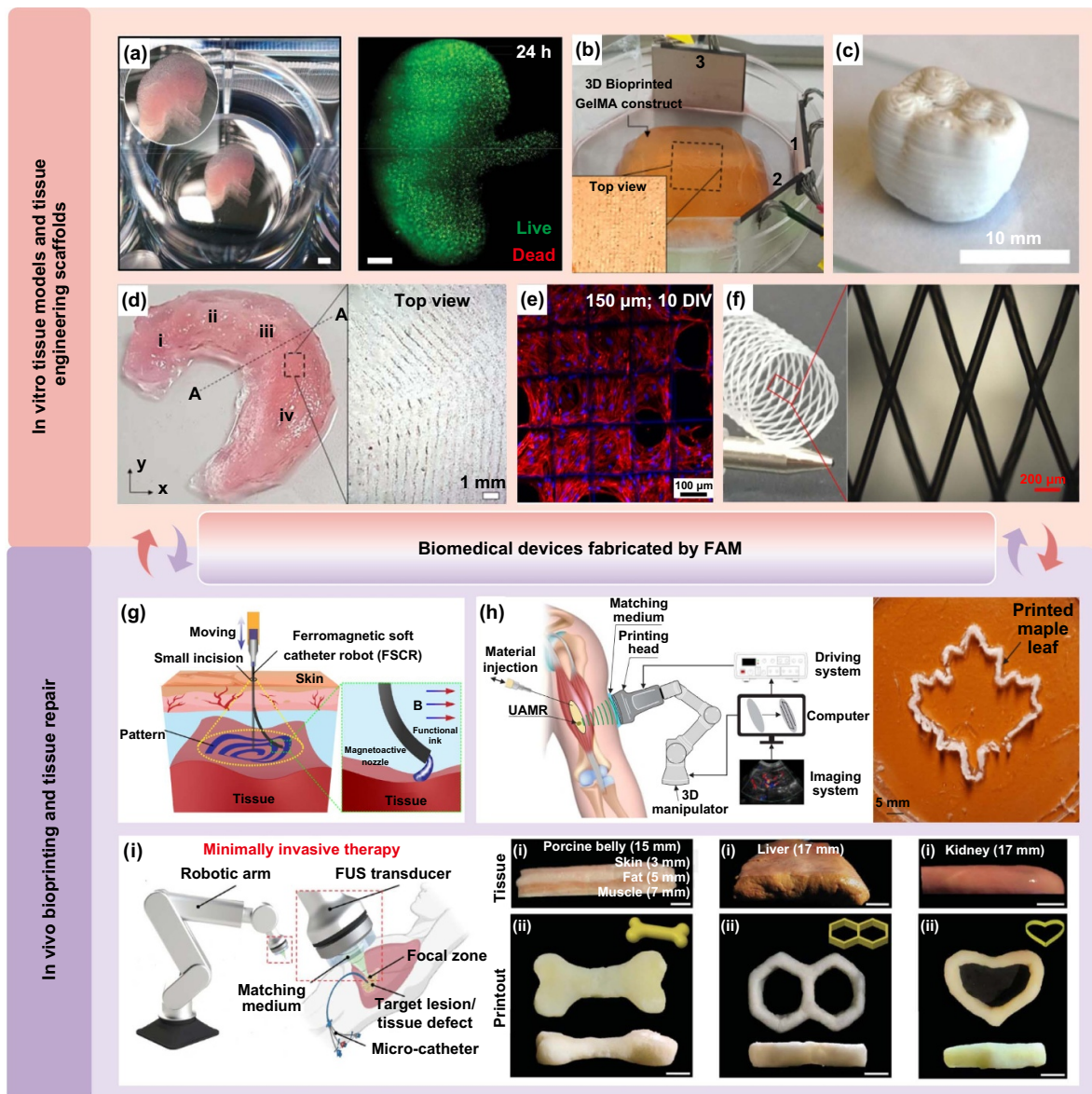


Figure 9. FAM for biomedical device applications. (a) Kidney-shaped hydrogel tissue model with high cellular viability. Reproduced from^[71], with permission from Springer Nature. (b) Microstructure with anisotropically aligned tendons and cardiac tissues. Reprinted from^[133], Copyright (2020), with permission from Elsevier. (c) Polymer crown model with submicron resolution. Reprinted from^[90], Copyright (2018), with permission from Elsevier. (d) Circumferential cell alignment in meniscus tissue. Reproduced from^[132]. © IOP Publishing Ltd. All rights reserved. (e) Submicron fiber scaffold with ultrafine filaments. Reproduced from^[165]. © IOP Publishing Ltd. CC BY 3.0. (f) Tubular mesh structure with 6 mm diameter and 80 μm linewidth. Reprinted from^[199], Copyright (2023), with permission from Elsevier. (g) Magnetic soft catheter robot achieving high-precision in vivo implant printing via superimposed magnetic fields. Reproduced from^[73]. CC BY 4.0. (h) Maple leaf pattern fabricated via focused ultrasound penetrative printing. Reproduced from^[148]. CC BY 4.0. (i) Deep-penetration acoustic volumetric printing for proof-of-concept validation and minimally invasive therapy via tissue printing. From^[149]. Reprinted with permission from AAAS.

microfluidic channels and cell patterning, advancing personalized drug screening (Figure 9(i))^[149].

In conclusion, FAM demonstrates its potential to overcome traditional limitations in resolution, material control, and biocompatibility, paving the way for innovative solutions in biomedical engineering, regenerative medicine, and personalized healthcare. By integrating magnetic, acoustic, and electric fields, FAM achieves unparalleled precision and functional

integration, positioning it as a transformative technology for next-generation micro/nano device fabrication.

3.3. Micro/nano electronic sensors

Micro/nano electronic sensors are pivotal in driving modern technological advancements and are extensively employed in health monitoring, environmental sensing, flexible electronics,

and intelligent microsystems. Operating at the micro- to nano-scale, these sensors demand exceptional precision in fabrication, stringent material compatibility, and intricate structural design^[150]. However, traditional micro/nano manufacturing techniques encounter significant limitations in achieving structural controllability, integrating diverse materials, and enabling scalable production. For instance, while photolithography excels in producing high-resolution micro/nano structures, its reliance on planar processing restricts the fabrication of complex 3D architectures, in addition to being cost-prohibitive^[200,201]. Similarly, chemical vapor deposition and physical vapor deposition excel in fabricating high-performance thin films but fall short in addressing heterogeneous integration and flexible substrate processing^[202,203]. Moreover, the growing demand for high sensitivity, stability, and rapid response in micro/nano electronic sensors presents additional challenges. Conventional methods struggle to precisely control the nanostructure of sensing layers, thereby limiting their application in trace-level signal detection and flexible device integration.

AFAM demonstrates remarkable advantages in the fabrication of conductive microcircuits. By leveraging acoustic radiation forces and soundwave-guided self-assembly effects, AFAM enables the precise arrangement of metallic nanoparticles or liquid metals on flexible substrates, forming uniform and highly stable conductive pathways. This approach significantly enhances both the reliability and electrical conductivity of microcircuits. Meanwhile, EFAM facilitates high-precision sensor fabrication through electric field-induced material deposition. Techniques such as EPD and EHDJ enable the controlled assembly and orientation of functional nanomaterials, such as graphene, optimizing sensor architectures and improving signal response characteristics. These advancements markedly enhance the detection sensitivity of physiological, electrochemical, and environmental signals.

In the field of microelectronic circuits, research focuses on achieving high-precision and multifunctional circuit designs through innovative manufacturing technologies. For instance, a 3D printing method combined with electroless deposition successfully printed an automatic LED switching system microcircuit directly onto 3D objects^[204]. This circuit exhibits excellent electrical conductivity, with low resistivity in its copper traces, ensuring efficient circuit operation. It is highly responsive to ambient light and can automatically regulate the switching of the LED based on ambient light intensity (Figure 10(a)). Moreover, it maintains stable performance even on curved substrates, highlighting its strong adaptability. To further expand applications on complex curved surfaces, electric-field-driven jetting was employed to print silver wires on a substrate inclined at 25° with a height difference of 10 mm^[68]. These silver wires exhibit excellent electrical conductivity, with a resistance of approximately 0.38 $\Omega \cdot \text{mm}^{-1}$, providing a reliable solution for the miniaturization and multifunctionalization of conformal circuits (Figure 10(b)). The introduction of acoustic field effects further enriches the design flexibility of conductive networks. By adjusting the acoustic focusing frequency, the conductive

properties of the microcircuit can be precisely controlled^[134]. For example, when the bundle spacing is 200 μm , the microcircuit can illuminate two 100 mA LEDs simultaneously; at 500 μm , only one LED lights up (Figure 10(c)).

Additionally, the advent of 4D printing technology brings more possibilities, such as a stretchable heating circuit based on fractal patterns, manufactured using electric-field-driven microscale 3D printing and integrated into a structure containing shape memory polymer components^[205]. The fifth-order Hilbert curve design of this circuit demonstrates high printing accuracy and complex design capabilities (Figure 10(d)), while exhibiting minimal resistance variation and efficient, uniform heating performance during stretching. A microcircuit micro-nano device containing a silver mesh was fabricated by combining electric field-driven microscale 3D printing technology with large-area imprinting technology. The silver mesh structure effectively promotes reflection, transmission, and multiple reflections of visible light and microwaves, thus realizing electromagnetic shielding (Figure 10(e))^[171].

In the field of micro/nano sensing, the research focus lies on developing self-powered and multifunctional sensors. For example, a P-TPMS lattice sensor fabricated using magnetic field-assisted photopolymerization 3D printing technology (Figure 10(f))^[101] converts mechanical compression into electrical signals, demonstrating excellent durability and adjustable sensitivity. After 10 000 compression cycles, the sensor's relative output voltage signal remains highly stable, and its sensitivity can be flexibly adjusted within the range of 0.75 $\mu\text{V} \cdot \text{mm}^{-1} \cdot \text{min}$ to 1.79 $\mu\text{V} \cdot \text{mm}^{-1} \cdot \text{min}$ by modifying the volume fraction of the P-TPMS lattice. Meanwhile, breakthroughs in the magneto-mechano-electric coupling effect have advanced the development of flexible tactile sensors. Researchers fabricated a tactile sensor using DIW combined with a magnetic-field-assisted folding magnetization method^[206], where the magnetic field signal exhibits a strong linear relationship (>0.98) with both the magnitude and position of the applied load. Fingertouch tests verified its high-resolution detection capability (Figure 10(g)). Furthermore, optimization of PVDF poling technology has significantly enhanced the performance of piezoelectric sensors. For instance, a flexible piezoelectric device generates an output current of approximately ± 1.5 nA and an electric charge of about 12.0 nC during manual bending and releasing (Figure 10(h))^[163]. Another force-sensing matrix based on PVDF integrates LEDs, adopting a sandwich structure design. A single sensor can illuminate different numbers of LEDs depending on the applied force, providing an intuitive real-time visualization of force changes (Figure 10(i))^[69]. This sensing matrix exhibits an average piezoelectric response of 47.76 $\text{pC} \cdot \text{N}^{-1}$, with loading and unloading response times of 98 ms and 68 ms, respectively, outperforming traditional unpolarized films.

AM, through the innovative integration of acoustic, electric, and magnetic field-assisted processes, has opened new pathways for microelectronic circuits and micro/nano sensing, breaking the limitations of traditional manufacturing. In the microelectronics domain, direct writing and particle

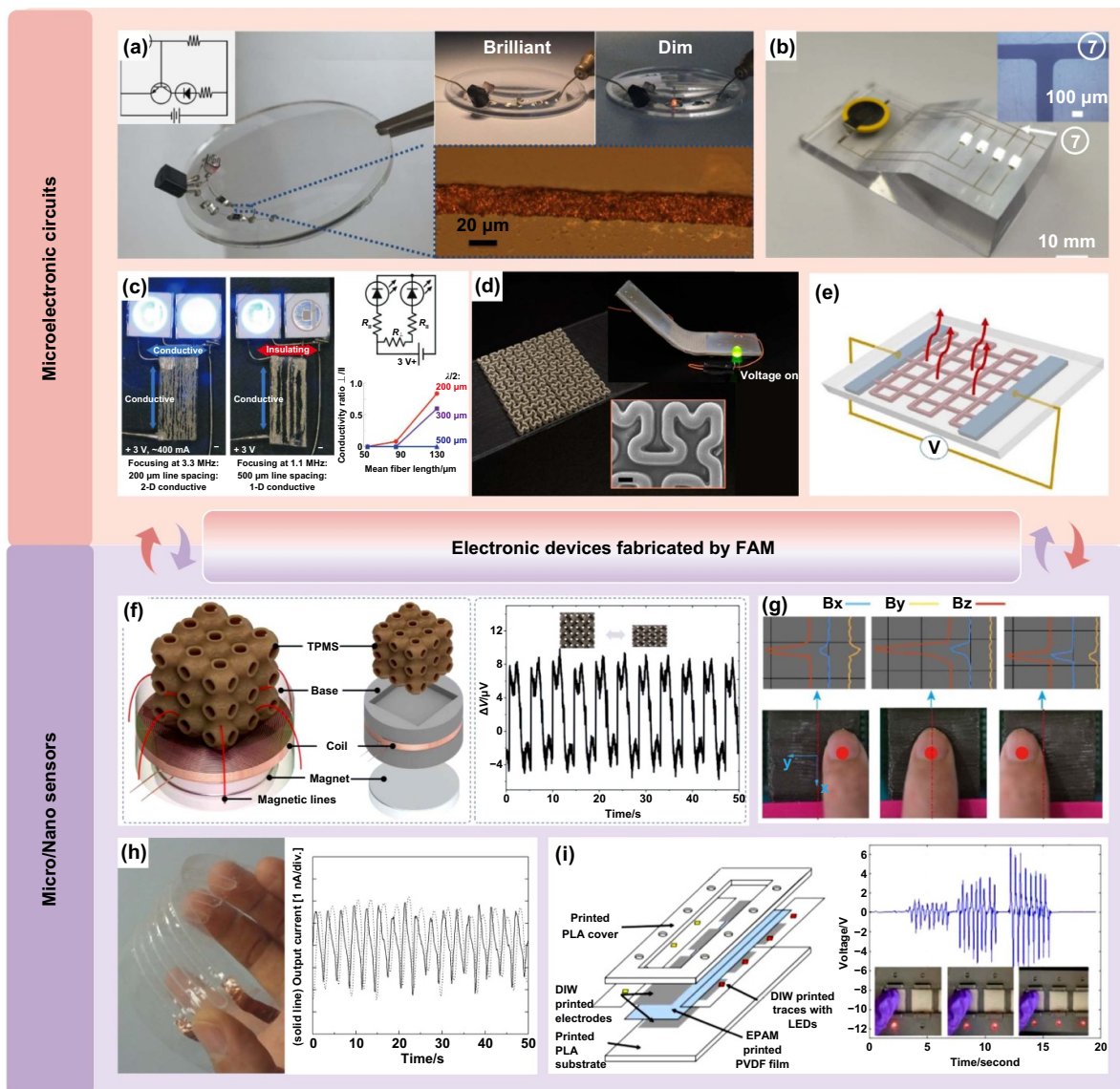


Figure 10. FAM for electronic sensor applications. (a) Direct printing of an automated LED switching system microcircuit onto 3D objects. Reprinted (adapted) with permission from^[204]. Copyright (2019) American Chemical Society. (b) Printing conductive silver traces on a substrate with a 25° tilt and a 10 mm height difference. Reprinted from^[68], Copyright (2024), with permission from Elsevier. (c) Conductive microcircuits with varying inter-trace spacing.^[134] John Wiley & Sons. © 2019 WILEY-VCH Verlag GmbH & Co. KGaA, Weinheim. (d) Stretchable heating circuits based on fractal-patterned structures. Reprinted (adapted) with permission from^[205]. Copyright (2021) American Chemical Society. (e) Embedded silver mesh with electromagnetic shielding functionality. Reprinted from^[171], Copyright (2023), with permission from Elsevier. (f) Self-powered multifunctional sensor based on P-TPMS lattice structures. Reproduced from^[101]. CC BY 4.0. (g) Magnetic tactile sensor. Reprinted from^[206], Copyright (2021), with permission from Elsevier. (h) Flexible piezoelectric sensor. Reproduced from^[163]. © IOP Publishing Ltd. All rights reserved. (i) PVDF-based force-sensing matrix. Reprinted from^[69], Copyright (2022), with permission from Elsevier.

self-assembly techniques enable high-precision fabrication of conformal circuits on complex curved surfaces, while fractal designs combined with shape memory polymers allow for the construction of stretchable electrothermal actuators. In the sensing domain, breakthroughs in magneto-mechano-electric coupling effects and PVDF poling technology have driven the practical application of self-powered sensors and high-sensitivity force-sensing matrices, surpassing the performance

metrics of conventional methods. These achievements validate the advantages of AFAM in the miniaturization and multifunctionalization of electronic devices and highlight its potential applications in robotics, wearable devices, and the Internet of Things. Future research needs to further optimize the synergistic effects of multiphysics fields to accelerate the scalable production of reliable, adaptive electronic devices.

4. Discussion and future trends

4.1. Discussion

Compared with traditional AM, FAM exhibits significant advantages in material manipulation, structural precision, and functionalization at the micro/nanoscale. By leveraging external fields, FAM enables precise control over material alignment, optimized material assembly, and ordered microstructure formation, which is critical for fabricating devices with anisotropic functionalities. For instance, MFAM facilitates the fabrication of magnetically responsive soft actuators by guiding magnetic particles to align along predefined orientations, thereby imparting unique magnetic and mechanical properties to the printed structures. Furthermore, FAM offers dynamic control over material spatial distribution, allowing devices to possess multiple functionalities post-fabrication. For example, AFAM employs acoustic radiation forces to precisely manipulate cell positioning, enabling the fabrication of highly organized 3D cellular scaffolds that promote cell proliferation and facilitate tissue engineering. Additionally, FAM overcomes material limitations in conventional AM, allowing precise processing of functional materials such as magnetic nanoparticles, conductive polymers, and bioactive materials, thereby expanding its applicability in smart microrobotics, flexible electronics, and biomedical devices. FAM presents immense potential in precise material arrangement, structural-functional optimization, and intelligent fabrication, offering a novel technological pathway for the development of next-generation high-performance MNDs.

Despite its immense potential in micro/nano manufacturing, FAM still faces several challenges to widespread adoption. Single external fields have been demonstrated to effectively manipulate material distribution, but limited attention has been given to their spatial uniformity. In MFAM, magnetic field generators typically produce non-uniform magnetic fields, which may lead to uneven material distribution, misalignment, and structural defects, ultimately affecting the precision and functionality of MNDs. Therefore, in the future, it is necessary to develop FAM equipment capable of generating highly uniform external fields to optimize the manufacturing precision of devices. However, although optimizing single external fields has significantly improved fabrication precision, the complexity of next-generation MNDs often demands multi-field coupled strategies. In many cases, a single external field struggles to meet the requirements of multi-scale control and multi-physics interactions, particularly in multifunctional electronic and biomedical applications.

Multi-field coupled manufacturing is quite complex in practical applications. This complexity is significantly amplified by potential interference or crosstalk between different field types and the challenges of integrating multiple field generation sources. Such integration within an AM system's confined space often requires specialized shielding and thermal management. Additionally, sophisticated and frequently custom-built control systems are needed. These systems must synchronize diverse field application parameters with the AM process in real-time. Furthermore, generating

different fields typically requires distinct types of generators, employing multiple generators to produce various fields can substantially reduce the available printable space and escalate control difficulty. Conversely, using a single device to generate multiple fields may introduce challenges such as asynchronous field application timing. Moreover, when multiple coupled fields assist in printing the same device, the behavior of particles within the device material is subjected to multiple field effects, potentially exhibiting unexpected arrangements. This necessitates adjusting the weighting of how various fields influence the material, thereby increasing control complexity. When multiple external fields act simultaneously, their interactions may induce nonlinear material responses, affecting the stability and predictability of the fabrication process. For example, the synergy between magnetic and electric fields can influence the orientation of conductive materials, potentially altering their electrical and mechanical performance. Similarly, combining acoustic and magnetic fields in biomedical device fabrication could impact cell alignment and differentiation, necessitating a deeper understanding of these interactions.

Furthermore, current FAM systems are predominantly laboratory-scale configurations, and their transition to industrial or clinical applications faces significant engineering and economic hurdles. Energy efficiency presents a major bottleneck, as the high-power consumption of field generators drives up operational costs and necessitates complex thermal management, particularly acute in large-scale production. Concurrently, the substantial initial investment required for specialized hardware, sophisticated control systems, and necessary shielding equipment constrains its economic viability.

To address these challenges, artificial intelligence (AI)-driven optimization and machine learning algorithms hold great promise for refining FAM strategies. By analyzing the dynamic evolution of materials under multi-field interactions, AI can enable real-time adjustments in process parameters, ensuring fabrication consistency and performance reliability. This integration of AI with FAM is expected to significantly enhance process stability, improve precision control, and unlock new possibilities for high-performance micro/nano device manufacturing.

4.2. Future trends

The rapid advancement of FAM has significantly driven innovations in micro/nano device fabrication. However, to facilitate its broader application across various fields, further improvements are required to enhance the stability of the manufacturing process, the level of intelligent control, and the scalability of production. Future developments in FAM are expected to focus on four key areas (Figure 11): (i) the development of highly uniform external field generation methods and advanced material distribution control techniques to improve the spatial precision and consistency of material manipulation; (ii) the optimization of multi-field coupling strategies to expand the manufacturability of MNDs through synergistic

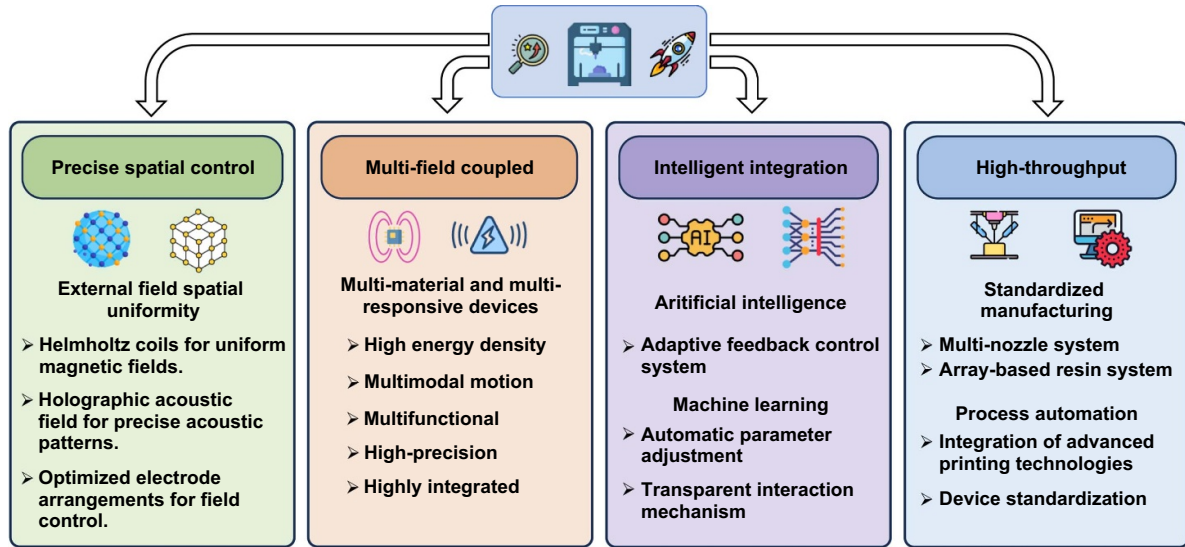


Figure 11. Further directions for FAM in micro/nano device fabrication.

interactions of multiple external fields; (iii) the intelligent integration of manufacturing processes by leveraging artificial intelligence and machine learning to enhance real-time process control; and (iv) breakthroughs in high-throughput manufacturing technologies to enable large-scale production of FAM-based devices. Progress in these areas is anticipated to further expand the applicability of FAM in micro/nano fabrication and provide a more advanced and well-established technological pathway to produce high-performance MNDs in the future.

4.2.1. Spatial precision control capability. Spatial precision control capability is essential for advancing FAM, as it determines the accuracy and functionality of MNDs. For magnetic fields, spatial non-uniformity can cause magnetic particles within the material to aggregate, resulting in non-uniform distribution and impaired device performance. Therefore, it is crucial to employ highly uniform magnetic fields during the printing process. The current trend involves the use of Helmholtz coils or Halbach arrays to generate controlled, uniform magnetic fields, enabling the fabrication of devices with homogeneous magnetization and superior functional properties. In the case of acoustic fields, achieving the required spatial precision is often challenged by wave reflections and interference from the boundaries of the printing chamber, which can disrupt the intended acoustic patterns and lead to field inhomogeneity at target locations. Overcoming this requires careful acoustic field design, advanced transducer arrangements, and real-time feedback control to ensure the desired spatial distribution of pressure nodes. For electric fields, spatial precision control focuses on generating well-defined field distributions that can align functional fillers and direct the assembly or deposition of materials at targeted locations. Non-uniform electric fields might lead to localized field enhancement, material breakdown, or uneven particle alignment, ultimately affecting the anisotropy and stability of the fabricated structures. The implementation of optimized

electrode configurations and adaptive voltage modulation is therefore necessary to achieve precise control of the electric field during fabrication.

4.2.2. Multi-field coupled manufacturing. Each FAM technique has unique advantages, and multi-field coupled AM offers expanded possibilities for micro/nano device fabrication. Alternating different FAM methods at various stages of the manufacturing process facilitates the construction of multi-material and multifunctional devices. For example, in micro/nanorobot fabrication, the coupling of magnetic and thermal fields can enhance material properties and increase energy density, while integration with electric fields can impart multi-responsive capabilities. Additionally, ultrasonic vibration effectively disperses aggregated particles within the printing material, improving particle uniformity in magnetically and electrically assisted manufacturing processes^[65,119,207]. Researchers have made significant progress in sub-diffraction and multi-photon lithography through the study of light field characteristics, and the integration with high-resolution EFAM offers the potential to achieve even greater manufacturing precision^[208]. Future advancements in multi-field coupled FAM are expected to drive the fabrication of high-precision, multifunctional MNDs, enhancing their integration and overall performance.

4.2.3. Intelligent control for process integration. FAM typically depends on pre-defined external field parameters, which poses challenges in adapting to dynamic changes in material states during the manufacturing process. Achieving closed-loop control is therefore essential for ensuring a reliable and repeatable FAM process. In particular, an effective closed-loop system should provide capabilities for real-time defect detection, fault analysis, and immediate regulation of process parameters to guarantee consistent product quality^[209]. With the rapid advancement of artificial intelligence (AI) and

machine learning (ML), there is a growing trend to leverage these technologies for real-time optimization and control of FAM. AI can be harnessed to develop adaptive feedback control systems that dynamically adjust printing parameters, such as external field direction, compensation voltage, and ultrasonic power intensity, in response to changes in key factors like particle loading rate and substrate tilt angle during fabrication^[68,137,168,210,211]. This approach helps to minimize manufacturing defects and improve precision.

Furthermore, integrating AI and ML with multi-physics simulations can accelerate the understanding of the complex interactive mechanisms in FAM, enabling more robust optimization of manufacturing strategies and process conditions^[212,213]. Intelligent integration of these technologies is expected to enhance the efficiency of FAM and push its evolution toward highly adaptive, intelligent manufacturing systems. This progress will lay a solid foundation for the large-scale and intelligent fabrication of complex micro/nanoscale devices based on FAM. Moreover, AI has demonstrated significant advantages not only in process monitoring and closed-loop control, but also in areas such as assisted design, material development, workflow management, and quality prediction across AM domains^[214]. In the future, the continued integration of AI with advanced feedback and control systems will enable more sophisticated monitoring, parameter optimization, and self-regulation. Ultimately, this will facilitate the transition of AM technologies from laboratory research to real-world industrial applications, supporting the vision of intelligent, automated manufacturing^[215].

4.2.4. High-throughput manufacturing. Currently, FAM remains primarily at the laboratory research stage, with its manufacturing speed and scalability still constrained. To enhance production efficiency, integrating multi-nozzle configurations or array-based resin reservoirs into existing systems can enable high-throughput parallel printing. Furthermore, the incorporation of intelligent external field regulation and real-time feedback control systems can optimize material deposition rates and precision while improving process consistency. Additionally, integrating FAM with advanced AM technologies is expected to overcome laboratory-scale limitations and accelerate its transition toward high-throughput manufacturing^[216,217]. In the future, achieving scalable FAM will require not only advancements in equipment and process optimization but also breakthroughs in material systems and automated control to expand its application potential.

5. Conclusion

This review provides a comprehensive summary of the research progress in FAM technologies, including magnetic, acoustic, and electric field-assisted methods, for micro/nano device fabrication. It first introduces the fundamental principles of FAM, focusing on the interaction mechanisms

between different external fields and materials, as well as their advantages in material alignment control, microstructure optimization, and functional enhancement under various manufacturing strategies (nozzle-based and VPP-based approaches). It then details the applications of FAM in fields such as micro/nanorobotics, biomedical devices, and micro/nano electronic sensors, highlighting specific studies that demonstrate its effectiveness in improving fabrication precision, enhancing material properties, and enabling multi-functionality. Furthermore, this review systematically compares the typical characteristics, representative applications, and unique advantages and limitations of MFAM, AFAM, and EFAM technologies, providing a clearer insight into their respective applicability and performance. Despite these advancements, FAM still faces several challenges, including the need for a deeper understanding of multi-field synergistic effects, improvements in process stability and reproducibility, and the expansion of its applicability to different material systems. Moving forward, FAM is expected to evolve toward intelligent manufacturing, multi-field synergy, and high-precision fabrication. The integration of AI and ML will enable adaptive manufacturing optimization, further enhancing printing accuracy and material control. Additionally, the synergistic use of multiple fields will improve manufacturing flexibility, allowing for the fabrication of more complex structures, while advancements in high-throughput manufacturing will facilitate the broader adoption of FAM in scalable production. Overall, FAM holds great potential in biomedical engineering, microelectronics, and intelligent manufacturing. The insights provided in this review, including discussions on current developments, challenges, and future directions, offer valuable guidance for future research and are expected to drive continued progress in high-performance micro/nano device fabrication.

Acknowledgments

The authors thank the financial support from the National Natural Science Foundation of China (Nos. 52205590, 52575652, 52322502, 52175009), State Key Laboratory of Robotics and Systems (HIT) (No. SKLRS-2024-KF-11), the Natural Science Foundation of Jiangsu Province (No. BK20220834), the Taihu Lake Innovation Fund for the School of Future Technology of Southeast University, the Start-up Research Fund of Southeast University (No. RF1028623098), the National Heilongjiang Providence Nature Science Foundation of China (YQ2022E022), and the European Research Council (ERC) under the European Union's Horizon Europe research and innovation programme (I-BOT Project, Grant Agreement No. 101162939).

ORCID iDs

Zhiyang Lyu  0000-0002-4305-4047

Tianlong Li  0000-0002-9483-457X

Qianqian Wang  0000-0001-8011-171X

References

- [1] Ceylan H, Giltinan J, Kozielski K and Sitti M. 2017. Mobile microrobots for bioengineering applications. *Lab Chip* **17**, 1705–1724.
- [2] Soto F, Wang J, Ahmed R and Demirci U. 2020. Medical micro/nanorobots in precision medicine. *Adv. Sci.* **7**, 2002203.
- [3] Barkam S, Saraf S and Seal S. 2013. Fabricated micro-nano devices for *in vivo* and *in vitro* biomedical applications. *WIREs Nanomed. Nanobiotechnol.* **5**, 544–568.
- [4] Zheng X R, Hu M S, Liu Y X, Zhang J, Li X, Li X and Yang H. 2022. High-resolution flexible electronic devices by electrohydrodynamic jet printing: from materials toward applications. *Sci. China Mater.* **65**, 2089–2109.
- [5] Wang X-X, Cao W-Q, Cao M-S and Yuan J. 2020. Assembling nano–microarchitecture for electromagnetic absorbers and smart devices. *Adv. Mater.* **32**, 2002112.
- [6] Nazemi H, Joseph A, Park J and Emadi A. 2019. Advanced micro- and nano-gas sensor technology: a review. *Sensors* **19**, 1285.
- [7] Li Y et al. 2025. Advanced multi-nozzle electrohydrodynamic printing: mechanism, processing, and diverse applications at micro/nano-scale. *Int. J. Extrem. Manuf.* **7**, 012008.
- [8] Wang Q Q, Zhang J C, Yu J F, Lang J, Lyu Z, Chen Y F and Zhang L. 2023. Untethered small-scale machines for microrobotic manipulation: from individual and multiple to collective machines. *ACS Nano* **17**, 13081–13109.
- [9] Wang Q Q and Zhang L. 2021. External power-driven microrobotic swarm: from fundamental understanding to imaging-guided delivery. *ACS Nano* **15**, 149–174.
- [10] Zhou H J, Mayorga-Martinez C C, Pané S, Zhang L and Pumera M. 2021. Magnetically driven micro and nanorobots. *Chem. Rev.* **121**, 4999–5041.
- [11] An C H, Wang T Y, Wu S, Gao L X, Deng Q B, Zhao L B and Hu N. 2023. Progress and prospective of the soft robots with the magnetic response. *Compos. Struct.* **324**, 117568.
- [12] Xiong J Y, Li X, He Z Y, Shi Y, Pan T, Zhu G S, Lu D Y and Xin H B. 2024. Light-controlled soft bio-microrobot. *Light Sci. Appl.* **13**, 55.
- [13] Limongi T, Tirinato L, Pagliari F, Giugni A, Allione M, Perozziello G, Candeloro P and Di Fabrizio E. 2017. Fabrication and applications of micro/nanostructured devices for tissue engineering. *Nano-Micro Lett.* **9**, 1.
- [14] Chen J L, Jin D D, Wang Q Q and Ma X. 2025. Programming ferromagnetic soft materials for miniature soft robots: design, fabrication, and applications. *J. Mater. Sci. Technol.* **219**, 271–287.
- [15] Huang Z Y, Shao G B and Li L Q. 2023. Micro/nano functional devices fabricated by additive manufacturing. *Prog. Mater. Sci.* **131**, 101020.
- [16] Zhang C Q, Li X J, Jiang L M, Tang D F, Xu H, Zhao P, Fu J Z, Zhou Q F and Chen Y. 2021. 3D printing of functional magnetic materials: from design to applications. *Adv. Funct. Mater.* **31**, 2102777.
- [17] Chen X-Z, Hoop M, Mushtaq F, Siringil E, Hu C Z, Nelson B J and Pané S. 2017. Recent developments in magnetically driven micro- and nanorobots. *Appl. Mater. Today* **9**, 37–48.
- [18] Jia B Q et al. 2024. Highly-sensitive, broad-range, and highly-dynamic MXene pressure sensors with multi-level nano-microstructures for healthcare and soft robots applications. *Chem. Eng. J.* **485**, 149750.
- [19] Liang X Y, Chen Z, Deng Y, Liu D, Liu X M, Huang Q and Arai T. 2023. Field-controlled microrobots fabricated by photopolymerization. *Cyborg Bionic Syst.* **4**, 0009.
- [20] Chen B, Sun H Y, Zhang J Y, Xu J J, Song Z Y, Zhan G D, Bai X and Feng L. 2024. Cell-based micro/nano-robots for biomedical applications: a review. *Small* **20**, 2304607.
- [21] Wang H P, Zhong S H, Zheng Z Q, Shi Q, Sun T, Huang Q and Fukuda T. 2024. Data-driven parallel adaptive control for magnetic helical microrobots with derivative structure in uncertain environments. *IEEE Trans. Syst. Man Cybern. Syst.* **54**, 4139–4150.
- [22] Onses M S, Sutanto E, Ferreira P M, Alleyne A G and Rogers J A. 2015. Mechanisms, capabilities, and applications of high-resolution electrohydrodynamic jet printing. *Small* **11**, 4237–4266.
- [23] Kong B, Liu R, Guo J H, Lu L, Zhou Q and Zhao Y J. 2023. Tailoring micro/nano-fibers for biomedical applications. *Bioact. Mater.* **19**, 328–347.
- [24] Li Y and Hong M H. 2020. Parallel laser micro/nano-processing for functional device fabrication. *Laser Photon. Rev.* **14**, 1900062.
- [25] Liu N, Wang F F, Liu L Q, Yu H B, Xie S R, Wang J, Wang Y C, Lee G-B and Li W J. 2016. Rapidly patterning micro/nano devices by directly assembling ions and nanomaterials. *Sci. Rep.* **6**, 32106.
- [26] Chen L S, Qiao W, Ye Y, Liu Y H and Pu D L. 2021. Critical technologies of micro-nano-manufacturing and its applications for flexible optoelectronic devices. *Acta Opt. Sin.* **41**, 0823018.
- [27] Leiterer C, Berg S, Jahr N, Brönstrup G, Christiansen S, Csaki A and Fritzsche W. 2011. Micronano integration of nanoscale objects for parallel biosensorics. *Proc. SPIE* **8068**, 80680W.
- [28] Liu Y, Li X T, Chen J and Yuan C L. 2020. Micro/nano electrode array sensors: advances in fabrication and emerging applications in bioanalysis. *Front. Chem.* **8**, 573865.
- [29] Jiang S L, Shi T L, Gao Y, Long H, Xi S and Tang Z R. 2014. Fabrication of a 3D micro/nano dual-scale carbon array and its demonstration as the microelectrodes for supercapacitors. *J. Micromech. Microeng.* **24**, 045001.
- [30] Liu J, Liang X X, Wang Y T, Wang B, Zhang T C and Yi F T. 2019. Fabrication and properties of micro-nano structure based heterojunction solar cell and photoresistor. *Mater. Res. Express* **6**, 075024.
- [31] He S K, Tian Y, Zhou H M, Zhu M M, Li C X, Fang B, Hong Z and Jing X F. 2025. Review for micro-nano processing technology of microstructures and metadevices. *Adv. Funct. Mater.* **35**, 2420369.
- [32] Kawata S, Sun H-B, Tanaka T and Takada K. 2001. Finer features for functional microdevices. *Nature* **412**, 697–698.
- [33] Al Noman A, Kumar B K and Dickens T. 2023. Field assisted additive manufacturing for polymers and metals: materials and methods. *Virtual Phys. Prototyp.* **18**, e2256707.
- [34] Safaee S, Schock M, Joyee E B, Pan Y Y and Chen R K. 2022. Field-assisted additive manufacturing of polymeric composites. *Addit. Manuf.* **51**, 102642.
- [35] Saadi M A S R, Maguire A, Pottackal N T, Thakur M S H, Ikram M M, Hart A J, Ajayan P M and Rahman M M. 2022. Direct ink writing: a 3D printing technology for diverse materials. *Adv. Mater.* **34**, 2108855.
- [36] Ma T B, Zhang Y L, Ruan K P, Guo H, He M K, Shi X T, Guo Y Q, Kong J and Gu J W. 2024. Advances in 3D printing for polymer composites: a review. *InfoMat* **6**, e12568.
- [37] Chen J, Virrueta C, Zhang S M, Mao C B and Wang J L. 2024. 4D printing: the spotlight for 3D printed smart materials. *Mater. Today* **77**, 66–91.
- [38] Ryan K R, Down M P and Banks C E. 2021. Future of additive manufacturing: overview of 4D and 3D printed smart and advanced materials and their applications. *Chem. Eng. J.* **403**, 126162.
- [39] Yang Y, Song X, Li X J, Chen Z Y, Zhou C, Zhou Q F and Chen Y. 2018. Recent progress in biomimetic additive manufacturing technology: from materials to functional structures. *Adv. Mater.* **30**, 1706539.

- [40] Jian B C, Li H G, He X N, Wang R, Yang H Y and Ge Q. 2024. Two-photon polymerization-based 4D printing and its applications. *Int. J. Extrem. Manuf.* **6**, 012001.
- [41] Ru C H, Luo J, Xie S R and Sun Y. 2014. A review of non-contact micro- and nano-printing technologies. *J. Micromech. Microeng.* **24**, 053001.
- [42] Park J-U et al. 2007. High-resolution electrohydrodynamic jet printing. *Nat. Mater.* **6**, 782–789.
- [43] Feng P, Yang F, Jia J Y, Zhang J, Tan W and Shuai C J. 2024. Mechanism and manufacturing of 4D printing: derived and beyond the combination of 3D printing and shape memory material. *Int. J. Extrem. Manuf.* **6**, 062011.
- [44] Lyu Z, Wang J L and Chen Y F. 2023. 4D printing: interdisciplinary integration of smart materials, structural design, and new functionality. *Int. J. Extrem. Manuf.* **5**, 032011.
- [45] Lyu Z et al. 2021. Design and manufacture of 3D-printed batteries. *Joule* **5**, 89–114.
- [46] Cao C et al. 2022. Dip-in photoresist for photoinhibited two-photon lithography to realize high-precision direct laser writing on wafer. *ACS Appl. Mater. Interfaces* **14**, 31332–31342.
- [47] Mueller P et al. 2017. Molecular switch for sub-diffraction laser lithography by photoenol intermediate-state cis–trans isomerization. *ACS Nano* **11**, 6396–6403.
- [48] Zhu D Z et al. 2022. Direct laser writing breaking diffraction barrier based on two-focus parallel peripheral-photoinhibition lithography. *Adv. Photon.* **4**, 066002.
- [49] Ryan K R, Down M P, Hurst N J, Keefe E M and Banks C E. 2022. Additive manufacturing (3D printing) of electrically conductive polymers and polymer nanocomposites and their applications. *eScience* **2**, 365–381.
- [50] Chen C, Wang X, Wang Y, Yang D D, Yao F Y, Zhang W X, Wang B, Sewvandi G A, Yang D S and Hu D W. 2020. Additive manufacturing of piezoelectric materials. *Adv. Funct. Mater.* **30**, 2005141.
- [51] Zhang N B et al. 2025. 3D printing of micro-nano devices and their applications. *Microsyst. Nanoeng.* **11**, 35.
- [52] Hu Y B. 2021. Recent progress in field-assisted additive manufacturing: materials, methodologies, and applications. *Mater. Horiz.* **8**, 885–911.
- [53] Tan C L et al. 2023. Review on field assisted metal additive manufacturing. *Int. J. Mach. Tool Manuf.* **189**, 104032.
- [54] Cao C et al. 2023. Cellulose derivative for biodegradable and large-scalable 2D nano additive manufacturing. *Addit. Manuf.* **74**, 103740.
- [55] Cao C, Xia X M, Shen X M, Wang X B, Yang Z Y, Liu Q L, Ding C L, Zhu D Z, Kuang C F and Liu X. 2024. Ultra-high precision nano additive manufacturing of metal oxide semiconductors via multi-photon lithography. *Nat. Commun.* **15**, 9216.
- [56] Cui H C et al. 2022. Design and printing of proprioceptive three-dimensional architected robotic metamaterials. *Science* **376**, 1287–1293.
- [57] Malley S, Newacheck S and Youssef G. 2021. Additively manufactured multifunctional materials with magnetoelectric properties. *Addit. Manuf.* **47**, 102239.
- [58] Johnson K, Melchert D, Gianola D S, Begley M and Ray T R. 2021. Recent progress in acoustic field-assisted 3D-printing of functional composite materials. *MRS Adv.* **6**, 636–643.
- [59] Kim Y, Yuk H, Zhao R K, Chester S A and Zhao X H. 2018. Printing ferromagnetic domains for untethered fast-transforming soft materials. *Nature* **558**, 274–279.
- [60] Hirt L, Reiser A, Spolenak R and Zambelli T. 2017. Additive manufacturing of metal structures at the micrometer scale. *Adv. Mater.* **29**, 1604211.
- [61] Kang K X, Liu Y B, Ren H S, Zhang Q H, Wang S Q, Kong Y N, Li W Y, Liu J R and Sun Q J. 2024. A novel magnetic field assisted powder arc additive manufacturing for Ti60 titanium alloy: method, microstructure and mechanical properties. *Addit. Manuf.* **83**, 104065.
- [62] Joyee E B, Szmelter A, Eddington D and Pan Y Y. 2020. Magnetic field-assisted stereolithography for productions of multimaterial hierarchical surface structures. *ACS Appl. Mater. Interfaces* **12**, 42357–42368.
- [63] Yunus D E, Sohrabi S, He R, Shi W T and Liu Y L. 2017. Acoustic patterning for 3D embedded electrically conductive wire in stereolithography. *J. Micromech. Microeng.* **27**, 045016.
- [64] Guo Y H, Batra S, Chen Y W, Wang E M and Cakmak M. 2016. Roll to roll electric field ‘Z’ alignment of nanoparticles from polymer solutions for manufacturing multifunctional capacitor films. *ACS Appl. Mater. Interfaces* **8**, 18471–18480.
- [65] Ansari M H D, Iacovacci V, Pane S, Ourak M, Borghesan G, Tamadon I, Vander Poorten E and Menciassi A. 2023. 3D printing of small-scale soft robots with programmable magnetization. *Adv. Funct. Mater.* **33**, 2211918.
- [66] Xu T Q, Zhang J C, Salehizadeh M, Onaizah O and Diller E. 2019. Millimeter-scale flexible robots with programmable three-dimensional magnetization and motions. *Sci. Robot.* **4**, eaav4494.
- [67] Sun H N et al. 2024. Magnetic field-assisted manufacturing of groove-structured flexible actuators with enhanced performance. *Addit. Manuf.* **80**, 103979.
- [68] Han Z F et al. 2024. High resolution conformal additive manufacturing based on electric-field-driven jet 3-axis micro-3D printing. *J. Manuf. Process.* **127**, 35–42.
- [69] Fan J S, Deneke N, Xu S J, Newell B, Garcia J, Davis C, Wu W Z, Voyles R M and Nawrocki R A. 2022. Electric poling-assisted additive manufacturing technique for piezoelectric active poly(vinylidene fluoride) films: towards fully three-dimensional printed functional materials. *Addit. Manuf.* **60**, 103248.
- [70] Xu K, Wang C T, Zhang Z X, Tang Y H and Guo H J. 2024. Flexible capacitive pressure sensor based on electrically assisted micro-nanoimprinting. *J. Mater. Sci.* **59**, 13575–13590.
- [71] Vidler C et al. 2024. Dynamic interface printing. *Nature* **634**, 1096–1102.
- [72] Xie R X et al. 2024. Magnetically driven formation of 3D freestanding soft bioscaffolds. *Sci. Adv.* **10**, ead11549.
- [73] Zhou C et al. 2021. Ferromagnetic soft catheter robots for minimally invasive bioprinting. *Nat. Commun.* **12**, 5072.
- [74] Jentsch S, Nasehi R, Kuckelkorn C, Gundert B, Aveic S and Fischer H. 2021. Multiscale 3D bioprinting by nozzle-free acoustic droplet ejection. *Small Methods* **5**, 2000971.
- [75] Li X Q, Zhang G M, Li W H, Yu Z, Yang K and Lan H B. 2020. The electric-field-driven fusion jetting 3d printing for fabricating high resolution polylactic acid/multi-walled carbon nanotube composite micro-scale structures. *Micromachines* **11**, 1132.
- [76] Fernandes Quero R, da Silveira G D, da Silva J A F and de Jesus D P D. 2021. Understanding and improving FDM 3D printing to fabricate high-resolution and optically transparent microfluidic devices. *Lab Chip* **21**, 3715–3729.
- [77] Sun Y X et al. 2023. 3D printing of thermosets with diverse rheological and functional applicabilities. *Nat. Commun.* **14**, 245.
- [78] Zhu X Y et al. 2019. Fabrication of high-performance silver mesh for transparent glass heaters via electric-field-driven microscale 3D printing and UV-assisted microtransfer. *Adv. Mater.* **31**, 1902479.
- [79] Schneider J, Rohner P, Thureja D, Schmid M, Galliker P and Poulidakos D. 2016. Electrohydrodynamic NanoDrip printing of high aspect ratio metal grid transparent electrodes. *Adv. Funct. Mater.* **26**, 833–840.

- [80] Lu L, Guo P and Pan Y Y. 2017. Magnetic-field-assisted projection stereolithography for three-dimensional printing of smart structures. *J. Manuf. Sci. Eng.* **139**, 071008.
- [81] Yang Y, Li X J, Chu M, Sun H F, Jin J, Yu K H, Wang Q M, Zhou Q F and Chen Y. 2019. Electrically assisted 3D printing of nacre-inspired structures with self-sensing capability. *Sci. Adv.* **5**, eaau9490.
- [82] Sanchez Noriega J L et al. 2021. Spatially and optically tailored 3D printing for highly miniaturized and integrated microfluidics. *Nat. Commun.* **12**, 5509.
- [83] Lichade K M, Hu S and Pan Y Y. 2023. Acoustic streaming-assisted two-photon polymerization process for the production of multimaterial microstructures. *Addit. Manuf.* **70**, 103552.
- [84] Shao G B, Ware H O T, Li L Q and Sun C. 2020. Rapid 3D printing magnetically active microstructures with high solid loading. *Adv. Eng. Mater.* **22**, 1900911.
- [85] Tumbleston J R et al. 2015. Continuous liquid interface production of 3D objects. *Science* **347**, 1349–1352.
- [86] Agrawal P et al. 2024. SonoPrint: acoustically assisted volumetric 3D printing for composites. *Adv. Mater.* **36**, 2408374.
- [87] Toombs J T, Luitz M, Cook C C, Jenne S, Li C C, Rapp B E, Kotz-Helmer F and Taylor H K. 2022. Volumetric additive manufacturing of silica glass with microscale computed axial lithography. *Science* **376**, 308–312.
- [88] Elder B, Neupane R, Tokita E, Ghosh U, Hales S and Kong Y L. 2020. Nanomaterial patterning in 3D printing. *Adv. Mater.* **32**, 1907142.
- [89] Yi H, Guo X Q, Chang F L, Cao H J, An J and Chua C K. 2025. Ink-jetting-based conformal additive manufacturing: advantages, opportunities, and challenges. *Int. J. Extrem. Manuf.* **7**, 032002.
- [90] Gunduz I E, McClain M S, Cattani P, Chiu G T C, Rhoads J F and Son S F. 2018. 3D printing of extremely viscous materials using ultrasonic vibrations. *Addit. Manuf.* **22**, 98–103.
- [91] Tee Y L, Tran P, Leary M, Pille P and Brandt M. 2020. 3D Printing of polymer composites with material jetting: mechanical and fractographic analysis. *Addit. Manuf.* **36**, 101558.
- [92] Rich J et al. 2024. Aerosol jet printing of surface acoustic wave microfluidic devices. *Microsyst. Nanoeng.* **10**, 2.
- [93] Ma T, Li Y, Cheng H, Niu Y J, Xiong Z X, Li A, Jiang X B, Park D, Zhang K F and Yi C L. 2024. Enhanced aerosol-jet printing using annular acoustic field for high resolution and minimal overspray. *Nat. Commun.* **15**, 6317.
- [94] Pagac M, Hajnys J, Ma Q-P, Jancar L, Jansa J, Stefek P and Mesicek J. 2021. A review of vat photopolymerization technology: materials, applications, challenges, and future trends of 3D printing. *Polymers* **13**, 598.
- [95] Pazhamannil R V and Govindan P. 2021. Current state and future scope of additive manufacturing technologies via vat photopolymerization. *Mater. Today Proc.* **43**, 130–136.
- [96] Medellin A, Du W C, Miao G X, Zou J, Pei Z J and Ma C. 2019. Vat photopolymerization 3D printing of nanocomposites: a literature review. *J. Micro Nano-Manuf.* **7**, 031006.
- [97] Karakurt I and Lin L W. 2020. 3D printing technologies: techniques, materials, and post-processing. *Curr. Opin. Chem. Eng.* **28**, 134–143.
- [98] Andreu A, Su P C, Kim J H, Ng C S, Kim S, Kim I, Lee J, Noh J, Subramanian A S and Yoon Y J. 2021. 4D printing materials for vat photopolymerization. *Addit. Manuf.* **44**, 102024.
- [99] Lichade K M and Pan Y Y. 2021. Acoustic field-assisted two-photon polymerization process. *J. Manuf. Sci. Eng.* **143**, 104501.
- [100] Meng X H, Li S S, Shen X J, Tian C Y, Mao L Y and Xie H. 2024. Programmable spatial magnetization stereolithographic printing of biomimetic soft machines with thin-walled structures. *Nat. Commun.* **15**, 10442.
- [101] Wu P, Yu T Y, Zhao L J and Chen M J. 2024. Magnetic field-assisted 3D printing of magnetic self-powered sensors. *Virtual Phys. Prototyp.* **19**, e2391487.
- [102] Zhai H R et al. 2024. 4D printing of Nd-Fe-B composites with both shape memory and permanent magnet excitation deformation. *Composites A* **187**, 108443.
- [103] Wei X X, Jin M L, Yang H Q, Wang X X, Long Y Z and Chen Z W. 2022. Advances in 3D printing of magnetic materials: fabrication, properties, and their applications. *J. Adv. Ceram.* **11**, 665–701.
- [104] Chaudhary V, Mantri S A, Ramanujan R V and Banerjee R. 2020. Additive manufacturing of magnetic materials. *Prog. Mater. Sci.* **114**, 100688.
- [105] Liu Y, Lin G G, Medina-Sánchez M, Guix M, Makarov D and Jin D Y. 2023. Responsive magnetic nanocomposites for intelligent shape-morphing microrobots. *ACS Nano* **17**, 8899–8917.
- [106] Kokkinis D, Schaffner M and Studart A R. 2015. Multimaterial magnetically assisted 3D printing of composite materials. *Nat. Commun.* **6**, 8643.
- [107] Roy M, Tran P, Dickens T and Quaipe B D. 2020. Effects of geometry constraints and fiber orientation in field assisted extrusion-based processing. *Addit. Manuf.* **32**, 101022.
- [108] Sun Y X, Wang L, Zhu Z Q, Li X X, Sun H, Zhao Y, Peng C H, Liu J, Zhang S W and Li M J. 2023. A 3D-printed ferromagnetic liquid crystal elastomer with programmed dual-anisotropy and multi-responsiveness. *Adv. Mater.* **35**, 2302824.
- [109] Song H, Spencer J, Jander A, Nielsen J, Stasiak J, Kasperchik V and Dhagat P. 2014. Inkjet printing of magnetic materials with aligned anisotropy. *J. Appl. Phys.* **115**, 17E308.
- [110] Zhou H X, Song C H, Yang Y Q, Han C J, Wang M, Xiao Y M and Liu Z X. 2022. The microstructure and properties evolution of SS316L fabricated by magnetic field-assisted laser powder bed fusion. *Mater. Sci. Eng. A* **845**, 143216.
- [111] Köhler J, Bösch W, Leitgeb E, Teschl R and Pommerenke D J. 2020. Manipulating iron filament with permanent magnets for FDM printing for X-band. In *2020 Int. Conf. on Broadband Communications for Next Generation Networks and Multimedia Applications (CoBCom)* (IEEE, Graz, Austria) pp 1–7.
- [112] Ahn T, Kim H-J, Lee J, Choi D-G, Jung J-Y, Choi J-H, Jeon S, Kim J-D and Jeong J-H. 2015. A facile patterning of silver nanowires using a magnetic printing method. *Nanotechnology* **26**, 345301.
- [113] Ansari M H D, Ha X T, Ourak M, Borghesan G, Iacovacci V, Vander Poorten E and Menciassi A. 2023. Characterization of a 3D printed endovascular magnetic catheter. *Actuators* **12**, 409.
- [114] Ma C P, Wu S, Ze Q, Kuang X, Zhang R D, Qi H J and Zhao R K. 2021. Magnetic multimaterial printing for multimodal shape transformation with tunable properties and shiftable mechanical behaviors. *ACS Appl. Mater. Interfaces* **13**, 12639–12648.
- [115] Martin J J, Caunter A, Dendulk A, Goodrich S, Pembroke R, Shores D and Erb R M. 2017. Direct-write 3D printing of composite materials with magnetically aligned discontinuous reinforcement. *Proc. SPIE* **10194**, 1019411.
- [116] Kummer M P, Abbott J J, Kratochvil B E, Borer R, Sengul A and Nelson B J. 2010. OctoMag: an electromagnetic system for 5-DOF wireless micromanipulation. *IEEE Trans. Robot.* **26**, 1006–1017.

- [117] Kim Y and Zhao X E. 2022. Magnetic soft materials and robots. *Chem. Rev.* **122**, 5317–5364.
- [118] Li X J et al. 2021. Limpet tooth-inspired painless microneedles fabricated by magnetic field-assisted 3D printing. *Adv. Funct. Mater.* **31**, 2003725.
- [119] Wu P, Yu T Y, Chen M J, Kang N and Mansori M E. 2024. Electrically/magnetically dual-driven shape memory composites fabricated by multi-material magnetic field-assisted 4D printing. *Adv. Funct. Mater.* **34**, 2314854.
- [120] Martin J J, Fiore B E and Erb R M. 2015. Designing bioinspired composite reinforcement architectures via 3D magnetic printing. *Nat. Commun.* **6**, 8641.
- [121] Huang Y J, Sun H N, Zhang C Q, Gao R X, Shen H Y and Zhao P. 2024. Multi-Material magnetic field-assisted additive manufacturing system for flexible actuators with programmable magnetic arrangements. *Front. Mech. Eng.* **19**, 16.
- [122] Zhou A W, Xu C Y, Kanitthamniyom P, Ng C S X, Lim G J, Lew W S, Vasoo S, Zhang X S, Lum G Z and Zhang Y. 2022. Magnetic soft millirobots 3D printed by circulating vat photopolymerization to manipulate droplets containing hazardous agents for in vitro diagnostics. *Adv. Mater.* **34**, 2200061.
- [123] Rasaki S A, Xiong D Y, Xiong S F, Su F, Idrees M and Chen Z W. 2021. Photopolymerization-based additive manufacturing of ceramics: a systematic review. *J. Adv. Ceram.* **10**, 442–471.
- [124] Huber C, Mitteramkogler G, Goertler M, Teliban I, Groenefeld M and Suess D. 2020. Additive manufactured polymer-bonded isotropic ndfeb magnets by stereolithography and their comparison to fused filament fabricated and selective laser sintered magnets. *Materials* **13**, 1916.
- [125] Safae S, Otero A, Fei M G, Liu T, Zhang J W and Chen R K. 2022. Particle-resin systems for additive manufacturing of rigid and elastic magnetic polymeric composites. *Addit. Manuf.* **51**, 102587.
- [126] Nagarajan B, Arshad M, Ullah A, Mertiny P and Qureshi A J. 2019. Additive manufacturing ferromagnetic polymers using stereolithography—materials and process development. *Manuf. Lett.* **21**, 12–16.
- [127] Guo Q, Su X, Zhang X G, Shao M C, Yu H X and Li D C. 2021. A review on acoustic droplet ejection technology and system. *Soft Matter* **17**, 3010–3021.
- [128] Sriphutkiat Y, Kasetsirikul S, Ketpun D and Zhou Y F. 2019. Cell alignment and accumulation using acoustic nozzle for bioprinting. *Sci. Rep.* **9**, 17774.
- [129] Sriphutkiat Y and Zhou Y F. 2017. Particle accumulation in a microchannel and its reduction by a standing surface acoustic wave (SSAW). *Sensors* **17**, 106.
- [130] Sriphutkiat Y, Kasetsirikul S and Zhou Y F. 2018. Formation of cell spheroids using Standing Surface Acoustic Wave (SSAW). *Int. J. Bioprinting* **4**, 130.
- [131] Chansoria P, Asif S, Gupta N, Piedrahita J and Shirwaiker R A. 2022. Multiscale anisotropic tissue biofabrication via bulk acoustic patterning of cells and functional additives in hybrid bioinks. *Adv. Healthcare Mater.* **11**, 2102351.
- [132] Chansoria P, Narayanan L K, Schuchard K and Shirwaiker R. 2019. Ultrasound-assisted biofabrication and bioprinting of preferentially aligned three-dimensional cellular constructs. *Biofabrication* **11**, 035015.
- [133] Chansoria P and Shirwaiker R. 2020. 3D bioprinting of anisotropic engineered tissue constructs with ultrasonically induced cell patterning. *Addit. Manuf.* **32**, 101042.
- [134] Melchert D S, Collino R R, Ray T R, Dolinski N D, Friedrich L, Begley M R and Gianola D S. 2019. Flexible conductive composites with programmed electrical anisotropy using acoustophoresis. *Adv. Mater. Technol.* **4**, 1900586.
- [135] Greenhall J and Raeymaekers B. 2017. 3D printing macroscale engineered materials using ultrasound directed self-assembly and stereolithography. *Adv. Mater. Technol.* **2**, 1700122.
- [136] Friedrich L, Collino R, Ray T and Begley M. 2017. Acoustic control of microstructures during direct ink writing of two-phase materials. *Sens. Actuators A* **268**, 213–221.
- [137] Wadsworth P, Nelson I, Porter D L, Raeymaekers B and Naleway S E. 2020. Manufacturing bioinspired flexible materials using ultrasound directed self-assembly and 3D printing. *Mater. Des.* **185**, 108243.
- [138] Liu C, Pandit P P, Parsons C, Khan F and Hu Y B. 2022. Acoustic field-assisted inkjet-based additive manufacturing of carbon fiber-reinforced polydimethylsiloxane composites. *J. Manuf. Process.* **80**, 87–94.
- [139] Foresti D, Kroll K T, Amisshah R, Sillani F, Homan K A, Poulidakos D and Lewis J A. 2018. Acoustophoretic printing. *Sci. Adv.* **4**, eaat1659.
- [140] Chen K K, Jiang E H, Wei X Y, Xia Y, Wu Z Z, Gong Z Y, Shang Z J and Guo S S. 2021. The acoustic droplet printing of functional tumor microenvironments. *Lab Chip* **21**, 1604–1612.
- [141] Niendorf K and Raeymaekers B. 2020. Quantifying macro- and microscale alignment of carbon microfibers in polymer-matrix composite materials fabricated using ultrasound directed self-assembly and 3D-printing. *Composites A* **129**, 105713.
- [142] Scholz M-S, Drinkwater B W and Trask R S. 2014. Ultrasonic assembly of anisotropic short fibre reinforced composites. *Ultrasonics* **54**, 1015–1019.
- [143] Li X W, Lim K M and Zhai W. 2022. A novel class of bioinspired composite via ultrasound-assisted directed self-assembly digital light 3D printing. *Appl. Mater. Today* **26**, 101388.
- [144] Zheng T F, Zheng X M, Wang Z Y, Shao M H, Liu X and Wang C H. 2024. Manufacturing of bioinspired Bouligand structures using ultrasound assisted 3D printing. *Sens. Actuators A* **372**, 115317.
- [145] Asif S, Chansoria P and Shirwaiker R. 2020. Ultrasound-assisted vat photopolymerization 3D printing of preferentially organized carbon fiber reinforced polymer composites. *J. Manuf. Process.* **56**, 1340–1343.
- [146] Xu C Y, Wang Y C, Pan H M, Li X and Mei D Q. 2024. Acoustic-assisted printing for polymer composites with programmable and regional microparticles patterning. *J. Manuf. Process.* **112**, 179–186.
- [147] Melde K, Choi E, Wu Z G, Palagi S, Qiu T and Fischer P. 2018. Acoustic fabrication via the assembly and fusion of particles. *Adv. Mater.* **30**, 1704507.
- [148] Habibi M, Foroughi S, Karamzadeh V and Packirisamy M. 2022. Direct sound printing. *Nat. Commun.* **13**, 1800.
- [149] Kuang X et al. 2023. Self-enhancing sono-inks enable deep-penetration acoustic volumetric printing. *Science* **382**, 1148–1155.
- [150] Criado-Gonzalez M, Dominguez-Alfaro A, Lopez-Larrea N, Alegret N and Mecerreyes D. 2021. Additive manufacturing of conducting polymers: recent advances, challenges, and opportunities. *ACS Appl. Polym. Mater.* **3**, 2865–2883.
- [151] Li Y L et al. 2025. Achieving impact-buffered compressible batteries through 3D printing-assisted design of negative Poisson's ratio structural electrodes. *Fundam. Res.* **5**, 2248–2255.
- [152] Plog J, Jiang Y, Pan Y and Yarin A L. 2021. Electrostatically-assisted direct ink writing for additive manufacturing. *Addit. Manuf.* **39**, 101644.
- [153] Rosenberger A G, Dragunski D C, Muniz E C, Módenes A N, Alves H J, Tarley C R T, Machado S A S and Caetano J.

2020. Electrospinning in the preparation of an electrochemical sensor based on carbon nanotubes. *J. Mol. Liq.* **298**, 112068.
- [154] Li H K et al. 2024. Directly printing high-resolution, high-performance 3D curved electronics based on locally polarized electric-field-driven vertical jetting. *Addit. Manuf.* **96**, 104579.
- [155] Vogt L, Schäfer M, Kurth D and Raether F. 2019. Usability of electrophoretic deposition for additive manufacturing of ceramics. *Ceram. Int.* **45**, 14214–14222.
- [156] Košir T and Slavič J. 2022. Single-process fused filament fabrication 3D-printed high-sensitivity dynamic piezoelectric sensor. *Addit. Manuf.* **49**, 102482.
- [157] Scott S M and Ali Z. 2021. Fabrication methods for microfluidic devices: an overview. *Micromachines* **12**, 319.
- [158] Yazdi A A, Popma A, Wong W, Nguyen T, Pan Y Y and Xu J. 2016. 3D printing: an emerging tool for novel microfluidics and lab-on-a-chip applications. *Microfluid. Nanofluid.* **20**, 50.
- [159] Mkhize N and Bhaskaran H. 2022. Electrohydrodynamic jet printing: introductory concepts and considerations. *Small Sci.* **2**, 2100073.
- [160] Ikram H, Al Rashid A and Koç M. 2022. Additive manufacturing of smart polymeric composites: literature review and future perspectives. *Polym. Compos.* **43**, 6355–6380.
- [161] Wei C and Dong J Y. 2014. Development and modeling of melt electrohydrodynamic-jet printing of phase-change inks for high-resolution additive manufacturing. *J. Manuf. Sci. Eng.* **136**, 061010.
- [162] Yang Y, Chen Z Y, Song X, Zhang Z F, Zhang J, Shung K K, Zhou Q F and Chen Y. 2017. Biomimetic anisotropic reinforcement architectures by electrically assisted nanocomposite 3D printing. *Adv. Mater.* **29**, 1605750.
- [163] Lee C and Tarbutton J A. 2014. Electric poling-assisted additive manufacturing process for PVDF polymer-based piezoelectric device applications. *Smart Mater. Struct.* **23**, 095044.
- [164] Keirouz A, Wang Z, Reddy V S, Nagy Z K, Vass P, Buzgo M, Ramakrishna S and Radacsi N. 2023. The history of electrospinning: past, present, and future developments. *Adv. Mater. Technol.* **8**, 2201723.
- [165] Hochleitner G, Jüngst T, Brown T D, Hahn K, Moseke C, Jakob F, Dalton P D and Groll J. 2015. Additive manufacturing of scaffolds with sub-micron filaments via melt electrospinning writing. *Biofabrication* **7**, 035002.
- [166] Li Z H et al. 2022. Directly printed embedded metal mesh for flexible transparent electrode via liquid substrate electric-field-driven jet. *Adv. Sci.* **9**, 2105331.
- [167] Jung W et al. 2021. Three-dimensional nanoprinting via charged aerosol jets. *Nature* **592**, 54–59.
- [168] Zhang G M, Lan H B, Qian L, Zhao J W and Wang F. 2020. A microscale 3D printing based on the electric-field-driven jet. *3D Print. Addit. Manuf.* **7**, 37–44.
- [169] Li J, Yang F, Long Y, Dong Y T, Wang Y Z and Wang X D. 2021. Bulk ferroelectric metamaterial with enhanced piezoelectric and biomimetic mechanical properties from additive manufacturing. *ACS Nano* **15**, 14903–14914.
- [170] Zhu X Y et al. 2021. Templateless, plating-free fabrication of flexible transparent electrodes with embedded silver mesh by electric-field-driven microscale 3D printing and hybrid hot embossing. *Adv. Mater.* **33**, 2007772.
- [171] Qi X M et al. 2023. Microscale hybrid 3D printed ultrahigh aspect ratio embedded silver mesh for flexible transparent electrodes. *Mater. Today Phys.* **33**, 101044.
- [172] Kirbus B, Brachmann E, Hengst C and Menzel S. 2018. Additive manufacturing of 96 MHz surface acoustic wave devices by means of superfine inkjet printing. *Smart Mater. Struct.* **27**, 075042.
- [173] Zhang G M et al. 2023. Electric-field-driven printed 3D highly ordered microstructure with cell feature size promotes the maturation of engineered cardiac tissues. *Adv. Sci.* **10**, 2206264.
- [174] Kim H, Torres F, Villagran D, Stewart C, Lin Y R and Tseng T-L B. 2017. 3D printing of BaTiO₃/PVDF composites with electric in situ poling for pressure sensor applications. *Macro Mater. Eng.* **302**, 1700229.
- [175] Pan Y Y, Patil A, Guo P and Zhou C. 2017. A novel projection based electro-stereolithography (PES) process for production of 3D polymer-particle composite objects. *Rapid Prototyp. J.* **23**, 236–245.
- [176] Pascall A J, Mora J, Jackson J A and Kuntz J D. 2015. Light directed electrophoretic deposition for additive manufacturing: spatially localized deposition control with photoconductive counter electrodes. *Key Eng. Mater.* **654**, 261–267.
- [177] Mora J, Dudoff J K, Moran B D, DeOtte J R, Du Frane W L, Kuntz J D and Pascall A J. 2018. Projection based light-directed electrophoretic deposition for additive manufacturing. *Addit. Manuf.* **22**, 330–333.
- [178] Zhong L P, Liu W, Sun Y Q, Wang F, Chen S, Sun Q Q, Liu Y F, Yuan C, Li X P and Fei G H. 2023. Electrically assisted stereolithography 3D printing of graded permittivity composites for in-situ encapsulation of insulated gate bipolar transistors (IGBTs). *Mater. Des.* **233**, 112220.
- [179] Zhang G M, Song D S, Jiang J, Li W H, Huang H, Yu Z, Peng Z L, Zhu X Y, Wang F and Lan H B. 2023. Electrically assisted continuous vat photopolymerization 3D printing for fabricating high-performance ordered graphene/polymer composites. *Composites B* **250**, 110449.
- [180] Liashenko I, Rosell-Llompart J and Cabot A. 2020. Ultrafast 3D printing with submicrometer features using electrostatic jet deflection. *Nat. Commun.* **11**, 753.
- [181] Wang Y C, Xu C Y, Liu J W, Pan H M, Li Y and Mei D Q. 2022. Acoustic-assisted 3D printing based on acoustofluidic microparticles patterning for conductive polymer composites fabrication. *Addit. Manuf.* **60**, 103247.
- [182] Wang Q Q, Chan K F, Schweizer K, Du X Z, Jin D D, Yu S C H, Nelson B J and Zhang L. 2021. Ultrasound Doppler-guided real-time navigation of a magnetic microswarm for active endovascular delivery. *Sci. Adv.* **7**, eabe5914.
- [183] Cao M M et al. 2024. Delivering microrobots in the musculoskeletal system. *Nano-Micro Lett.* **16**, 251.
- [184] Zhong S H, Xin Z Y, Hou Y Z, Li Y, Huang H W, Sun T, Shi Q and Wang H P. 2024. Double-modal locomotion of a hydrogel ultra-soft magnetic miniature robot with switchable forms. *Cyborg Bionic Syst.* **5**, 0077.
- [185] Koleoso M, Feng X, Xue Y, Li Q, Munshi T and Chen X. 2020. Micro/nanoscale magnetic robots for biomedical applications. *Mater. Today Bio* **8**, 100085.
- [186] Deng Y, Paskert A, Zhang Z Y, Wittkowski R and Ahmed D. 2023. An acoustically controlled helical microrobo. *Sci. Adv.* **9**, eadh5260.
- [187] Wang Q L et al. 2024. Tracking and navigation of a microswarm under laser speckle contrast imaging for targeted delivery. *Sci. Robot.* **9**, eadh1978.
- [188] Wang B et al. 2024. tPA-anchored nanorobots for in vivo arterial recanalization at submillimeter-scale segments. *Sci. Adv.* **10**, eadh8970.
- [189] Li Q W, Niu F Z, Yang H, Xu D Q, Dai J, Li J, Chen C S, Sun L N and Zhang L. 2024. Magnetically actuated soft microrobot with environmental adaptative multimodal locomotion towards targeted delivery. *Adv. Sci.* **11**, 2406600.
- [190] Chen Y Y, Chen D, Liang S, Dai Y, Bai X, Song B, Zhang D, Chen H and Feng L. 2022. Recent advances in field-controlled micro–nano manipulations and micro–nano robots. *Adv. Intell. Syst.* **4**, 2100116.

- [191] Wallin T J, Pikul J and Shepherd R F. 2018. 3D printing of soft robotic systems. *Nat. Rev. Mater.* **3**, 84–100.
- [192] Kaynak M, Dirix P and Sakar M S. 2020. Addressable acoustic actuation of 3D printed soft robotic microsystems. *Adv. Sci.* **7**, 2001120.
- [193] Ren Z Y and Sitti M. 2024. Design and build of small-scale magnetic soft-bodied robots with multimodal locomotion. *Nat. Protocols* **19**, 441–486.
- [194] Zhou S, Li Y H, Wang Q Q and Lyu Z. 2024. Integrated actuation and sensing: toward intelligent soft robots. *Cyborg Bionic Syst.* **5**, 0105.
- [195] Han W H, Gao W and Wang X Z. 2024. Enhanced magnetic soft robotics: integrating fiber optics and 3D printing for rapid actuation and precision sensing. *ACS Appl. Mater. Interfaces* **16**, 30396–30407.
- [196] Li Z X, Lai Y P and Diller E. 2024. 3D printing of multilayer magnetic miniature soft robots with programmable magnetization. *Adv. Intell. Syst.* **6**, 2300052.
- [197] Zhang L W et al. 2023. A magnetic-driven multi-motion robot with position/orientation sensing capability. *Research* **6**, 0177.
- [198] Chen J S, Chen J B, Wang H Z, He L, Huang B Y, Dadbakhsh S and Bartolo P. 2025. Fabrication and development of mechanical metamaterials via additive manufacturing for biomedical applications: a review. *Int. J. Extrem. Manuf.* **7**, 012001.
- [199] Peng Z L et al. 2023. Electric field-driven microscale 3D printing of flexible thin-walled tubular mesh structures of molten polymers. *Mater. Des.* **225**, 111433.
- [200] Liu J S, Guo H J, Li M, Zhang C, Chu Y Z, Che L X, Zhang Z H, Li R, Sun J N and Lu Y. 2021. Photolithography-assisted precise patterning of nanocracks for ultrasensitive strain sensors. *J. Mater. Chem. A* **9**, 4262–4272.
- [201] Bathaei M J, Singh R, Mirzajani H, Istif E, Akhtar M J, Abbasiasl T and Beker L. 2023. Photolithography-based microfabrication of biodegradable flexible and stretchable sensors. *Adv. Mater.* **35**, 2207081.
- [202] Kumar R, Goel N, Kumar Jarwal D, Hu Y H, Zhang J and Kumar M. 2023. Strategic review on chemical vapor deposition technology-derived 2D material nanostructures for room-temperature gas sensors. *J. Mater. Chem. C* **11**, 774–801.
- [203] Chu J, Peng X Y, Feng P, Sheng Y and Zhang J T. 2013. Study of humidity sensors based on nanostructured carbon films produced by physical vapor deposition. *Sens. Actuators B* **178**, 508–513.
- [204] Lee S, Wajahat M, Kim J H, Pyo J, Chang W S, Cho S H, Kim J T and Seol S K. 2019. Electroless deposition-assisted 3D printing of micro circuitries for structural electronics. *ACS Appl. Mater. Interfaces* **11**, 7123–7130.
- [205] Zhang Y-F, Li Z H, Li H K, Li H G, Xiong Y, Zhu X Y, Lan H B and Ge Q. 2021. Fractal-based stretchable circuits via electric-field-driven microscale 3D printing for localized heating of shape memory polymers in 4D printing. *ACS Appl. Mater. Interfaces* **13**, 41414–41423.
- [206] Zhang X C, Hu H, Tang D F, Zhang C Q, Fu J Z and Zhao P. 2021. Magnetic flexible tactile sensor via direct ink writing. *Sens. Actuators A* **327**, 112753.
- [207] Bao Y W, Li J, Wang T, Wang L and Xu H. 2024. Photothermal programming of magnetic soft materials for complex and reconfigurable 3D deformations. *Sci. China Mater.* **67**, 4031–4039.
- [208] Guan L L et al. 2024. Light and matter co-confined multi-photon lithography. *Nat. Commun.* **15**, 2387.
- [209] Fang Q H, Xiong G, Zhou M C, Tamir T S, Yan C-B, Wu H Y, Shen Z and Wang F-Y. 2024. Process monitoring, diagnosis and control of additive manufacturing. *IEEE Trans. Autom. Sci. Eng.* **21**, 1041–1067.
- [210] Patton M V, Ryan P, Calascione T, Fischer N, Morgenstern A, Stenger N and Nelson-Cheeseman B B. 2019. Manipulating magnetic anisotropy in fused filament fabricated parts via macroscopic shape, mesoscopic infill orientation, and infill percentage. *Addit. Manuf.* **27**, 482–488.
- [211] Lu L, Baynoji Joyee E and Pan Y Y. 2018. Correlation between microscale magnetic particle distribution and magnetic-field-responsive performance of three-dimensional printed composites. *J. Micro Nano-Manuf.* **6**, 010904.
- [212] Liu C N, Tian W M and Kan C. 2022. When AI meets additive manufacturing: challenges and emerging opportunities for human-centered products development. *J. Manuf. Syst.* **64**, 648–656.
- [213] Ng W L, Goh G L, Goh G D, Ten J S J and Yeong W Y. 2024. Progress and opportunities for machine learning in materials and processes of additive manufacturing. *Adv. Mater.* **36**, 2310006.
- [214] Gu S, Choi M, Park H, Jeong S, Doh J and Park S-I. 2023. Application of artificial intelligence in additive manufacturing. *JMST Adv.* **5**, 93–104.
- [215] Sani A R, Zolfagharian A and Kouzani A Z. 2024. Artificial intelligence-augmented additive manufacturing: insights on closed-loop 3D printing. *Adv. Intell. Syst.* **6**, 2400102.
- [216] Regehly M, Garmshausen Y, Reuter M, König N F, Israel E, Kelly D P, Chou C-Y, Koch K, Asfari B and Hecht S. 2020. Xolography for linear volumetric 3D printing. *Nature* **588**, 620–624.
- [217] Kronenfeld J M, Rother L, Saccone M A, Dulay M T and DeSimone J M. 2024. Roll-to-roll, high-resolution 3D printing of shape-specific particles. *Nature* **627**, 306–312.